The Lagrangian particle dispersion model FLEXPART version 10.3

Ignacio Pisso[1], Espen Sollum[1], Henrik Grythe[1], Nina I. Kristiansen[1,*], Massimo Cassiani[1], Sabine Eckhardt[1], Delia Arnold[2,3], Don Morton[4], Rona L. Thompson[1], Cristine D. Groot Zwaaftink[1], Nikolaos Evangeliou[1], Harald Sodemann[5], Leopold Haimberger[6], Stephan Henne[7], Dominik Brunner[7], John F. Burkhart[8], Anne Fouilloux[8], Jerome Brioude[9], Anne Philipp[6,10], Petra Seibert[11], and Andreas Stohl[1]

[1]Norwegian Institute of Air Research, Kjeller, Norway
[2]Central Institute for Meteorology and Geodynamics, Vienna, Austria.
[3]Arnold Scientific Consulting, Manresa, Spain
[4]Boreal Scientific Computing, Fairbanks, Alaska, USA
[5]Geophysical Institute, University of Bergen, Norway
[6]Department of Meteorology and Geophysics, University of Vienna, Austria
[7]EMPA, Dübendorf, Switzerland
[8]Department of Geosciences, University of Oslo, Norway
[9]LACy, Université de la Réunion, France
[10]Aerosol Physics & Environmental Physics, University of Vienna, Austria
[11]University of Natural Resources and Life Sciences, Institute of Meteorology, Vienna, Austria
[*]now at Met Office, FitzRoy Road, Exeter, EX1 3PB, UK

Abstract. The Lagrangian particle dispersion model FLEXPART was in its original version in the mid-1990s designed for calculating the long-range and mesoscale dispersion of hazardous substances from point sources, such as released after an accident in a nuclear power plant. Over the past decades, the model has evolved into a comprehensive tool for multi-scale atmospheric transport modelling and analysis and has attracted a global user community. Its application fields have been extended to a large

5   range of atmospheric gases and aerosols, e.g. greenhouse gases, short-lived climate forcers like black carbon, or volcanic emissions, and it has also been used to study the atmospheric branch of the water cycle. Given suitable meteorological input data, it can be used for scales from dozens of meters to the global scale. In particular, inverse modelling based on source-receptor relationships from FLEXPART has become widely used. In this paper, we present FLEXPART version 10.3, which works with meteorological input data from the European Centre for Medium-Range Weather Forecasts' (ECMWF) Integrated Forecast

10   System (IFS), and data from the United States' National Centers of Environmental Prediction (NCEP) Global Forecast System (GFS). Since the last publication of a detailed FLEXPART description (version 6.2), the model has been improved in different aspects such as performance, physico-chemical parametrizations, input/output formats and available pre- and post-processing software. The model code has also been parallelized using the Message Passing Interface (MPI). We demonstrate that the model scales well up to using 256 processors, with a parallel efficiency greater than 75% for up to 64 processes on multiple nodes.

15   The deviation from 100% efficiency is almost entirely due to remaining non-parallelized parts of the code, suggesting large potential for further speed-up. A new turbulence scheme for the convective boundary layer has been developed that considers the skewness in the vertical velocity distribution (updrafts and downdrafts) and vertical gradients in air density. FLEXPART is the only model available considering both effects, making it highly accurate for small-scale applications, e.g. to quantify

dispersion in the vicinity of a point source. The wet deposition scheme for aerosols has been completely rewritten and a new, more detailed gravitational settling parameterization for aerosols has also been implemented. FLEXPART has had the option for running backward in time from atmospheric concentrations at receptor locations since many years, but this has now been extended to work also for deposition values and may become useful, for instance, for the interpretation of ice core measure-

5 ments. To our knowledge, to date FLEXPART is the only model with that capability. Furthermore, temporal variation and temperature dependence of chemical reactions with the OH radical have been included, allowing more accurate simulations for species with intermediate lifetimes against the reaction with OH, such as ethane. Finally, user settings can now be specified in a more flexible namelist format, and output files can be produced in NetCDF format instead of FLEXPART's customary binary format. In this paper, we describe these new developments. Moreover, we present some tools for the preparation of the

10 meteorological input data and for processing of FLEXPART output data and briefly report on alternative FLEXPART versions.

Contents

1 Introduction

Multi-scale off-line Lagrangian particle dispersion models (LPDMs) are versatile tools for simulating the transport and turbulent mixing of gases and aerosols in the atmosphere. Examples of such models are the Numerical Atmospheric-dispersion Modelling Environment (NAME) (Jones et al. , 2007), the Stochastic Time-Inverted Lagrangian Transport (STILT) model

10 (Lin et al., 2003), the Hybrid Single-Particle Lagrangian Integrated Trajectory (HYSPLIT) model (Stein et al., 2015), and the FLEXible PARTicle (FLEXPART) model (Stohl et al., 1998, 2005). LPDMs are stochastic models that compute the trajectories for a large number of notional particles that do not represent real aerosol particles but points moving with the ambient flow. The trajectories represent the transport by the mean flow as well as turbulent, diffusive transport by unresolved parameterized sub-grid scale transport processes (e.g. turbulence, meandering, deep convection, etc.) and can also include gravitational set-

15 tling. Each particle carries a certain mass, which can be affected by loss processes such as radioactive decay, chemical loss or dry and wet deposition.

The theoretical basis for most currently used atmospheric particle models was laid down by Thomson (1987). He introduced the criterion to formulate Lagrangian stochastic models that produce particle trajectories consistent with pre-defined Eulerian probability density functions in physical and velocity space. Rodean (1996) and Wilson and Sawford (1996) provided detailed

20 descriptions of the theory and formulation of LPDMs in constant-density flows and under different atmospheric stability conditions. Stohl and Thomson (1999) extended this to flows with vertically variable air density. An important characteristic of LPDMs is their ability to run backward in time in a framework that is theoretically consistent with both the Eulerian flow field and LPDM forward calculations. This was discussed by Thomson (1987, 1990), further developed by Flesch et al. (1995), and extended to global scale dispersion by Stohl et al. (2003) and Seibert and Frank (2004). The more practical aspects and

25 efficiency of LPDMs were discussed by Zannetti (1992) and Uliasz (1994). A history of their development was provided by Thomson and Wilson (2013).

Lagrangian models exhibit much less numerical diffusion than Eulerian or semi-Lagrangian models (e.g. Reithmeier and Sausen, 2002; Cassiani et al., 2016), even though some artificial numerical errors arise also in the discretization of their stochastic differential equations (Ramli and Esler, 2016). Due to their low level of numerical diffusion, tracer filaments gen-

30 erated by the dispersion in the atmosphere (Ottino, 1989) are much better captured in Lagrangian models than in Eulerian models. It has been noticed, for instance, that Eulerian models have difficulties simulating the fine tracer structures created by intercontinental pollution transport (Rastigejev et al., 2010), while these are well preserved in LPDMs (e.g. Stohl et al., 2003). Furthermore, in Eulerian models a tracer released from a point source is instantaneously mixed within a grid box, whereas

Lagrangian models are independent of a computational grid and can account for point or line sources with potentially infinitesimal spatial resolution. When combined with their capability to run backward in time, this means that LPDMs can also be used to reconstruct the air history of atmospheric point measurements (e.g. in-situ measurements of atmospheric composition).

The computational efficiency of LPDMs depends on the type of application. One important aspect is that their computa-
5   tional cost does not increase substantially with the number of species transported (excluding aerosol particles with different gravitational settling, for which trajectories deviate from each other), making multi-species simulations efficient. On the other hand, the computational time scales linearly with the number of particles used, while the statistical error in the model output decreases only with the square root of the particle density. Thus, it can be computationally costly to reduce statistical errors, and data input/output can require substantial additional resources. Generally, a high particle density can be achieved with a
10 small number of released particles in the vicinity of a release location, where statistical errors, relative to simulated concentrations, are typically small. However, particle density and thus the relative accuracy of the results decreases with distance from the source. Methods should therefore be used to reduce the statistical error (e.g. Heinz et al., 2003), such as kernels or particle splitting, and it is important to quantify the statistical error.

1.1 The Lagrangian particle dispersion model FLEXPART

15 One of the most widely used LPDMs is the open-source model FLEXPART, which simulates the transport, diffusion, dry and wet deposition, radioactive decay and first order chemical reactions (e.g. OH oxidation) of tracers released from point, line, area or volume sources, or filling the whole atmosphere (Stohl et al., 1998, 2005). FLEXPART development started more than two decades ago (Stohl et al., 1998) and the model has been free software ever since it was first released. The status as a free software is formally established by releasing the code under the GNU General Public License (GPL) Version 3. However, the
20 last peer-reviewed publication describing FLEXPART (version 6.2) was published as a technical note about 14 years ago (Stohl et al., 2005). Since then, while updates of FLEXPART's source code and a manual were made available from the web page https://flexpart.eu/, no citable reference was provided. In this paper, we describe FLEXPART developments since Stohl et al. (2005), which led to the current version 10.3 (subsequently abbreviated as v10.3).

FLEXPART can be run either forward or backward in time. For forward simulations, particles are released from one or more
25 sources and concentrations (or mixing ratios) are determined on a regular latitude-longitude-altitude grid. In backward mode, the location where particles are released represents a receptor (e. g. a measurement site). Like in the forward mode, particles are sampled on a latitude-longitude-altitude grid, which in this case corresponds to potential sources. The functional values obtained represent the source-receptor relationship (SRR) (Seibert and Frank, 2004), also called source-receptor sensitivity (Wotawa et al., 2003) or simply emission sensitivity, and are related to the particles' residence time in the output grid cells.
30 Backward modelling is more efficient than forward modelling for calculating SRRs if the number of receptors is smaller than the number of (potential) sources. Seibert and Frank (2004) explained in detail the theory of backward modelling, and Stohl et al. (2003) gave a concrete backward modelling example. FLEXPART can also be used in a domain-filling mode where the entire atmosphere is represented by particles of equal mass (Stohl and James, 2004).

FLEXPART is an off-line model that uses meteorological fields (analyses or forecasts) as input. Such data are available from several different numerical weather prediction (NWP) models. For the model version described here, v10.3, data from the European Centre for Medium-Range Weather Forecasts' (ECMWF) Integrated Forecast System (IFS), and data from the United States' National Centers of Environmental Prediction's (NCEP) Global Forecast System (GFS) can be used. Other
5 FLEXPART model branches have been developed for input data from various limited-area models, for example the Weather Research and Forecasting (WRF) meteorological model (Brioude et al., 2013) or the Consortium for Small-scale Modeling (COSMO) model (Oney, 2015) which extend the applicability of FLEXPART down to the meso-gamma scale. Notice that the turbulence parameterizations of FLEXPART are valid at even smaller scales. Another FLEXPART model version, FLEXPART-NorESM/CAM (Cassiani et al., 2016) uses the meteorological output data generated by the Norwegian Earth System Model
10 (NorESM1-M) with its atmospheric component CAM (Community Atmosphere Model). The current paper does not document these other model branches, but most share many features with FLEXPART v10.3 and some are briefly described in appendix C. A key aspect of these model branches is the ability to read meteorological input other than from ECMWF or NCEP.

1.2 FLEXPART and its history

FLEXPART's first version (v1) was a further development of the trajectory model FLEXTRA (Stohl et al., 1995) and was
15 coded in Fortran 77. It provided gridded output of concentrations of chemical species and radionuclides. Its input data were based on ECMWF's specific GRIB-1 (Gridded Binary) format. The model was first applied in an extensive validation study using measurements from three large scale tracer experiments (Stohl et al., 1998). A deposition module was added in version 2. Version 3 saw improvements in performance and the addition of a subgrid scale terrain effects parametrization. In v3.1 the output format was optimized (sparse matrix) and mixing ratio output could optionally be produced. It also allowed the output
20 of particle positions. Furthermore, a density correction was added to account for decreasing air density with height in the boundary layer (Stohl and Thomson, 1999). Further v3 releases included the addition of a convection scheme (Seibert et al., 2001), the option to calculate mass fluxes across grid cell center lines and age spectra, and free format input (v3.2). The preliminary convection scheme of v3.2 was replaced by the convection scheme of Emanuel and Živković-Rothman (1999) in v4 (see Forster et al., 2007). In v5 the unit of the backward calculation was changed to seconds and improvements in the input/output
25 handling were made. Comprehensive validation of these early FLEXPART versions was done during intercontinental air pollution transport studies at the end of the 1990s and early 2000s (Stohl and Trickl, 1999; Forster et al., 2001; Spichtinger et al., 2001; Stohl et al., 2002, 2003). Special developments were also made in order to extend FLEXPART's forecasting capabilities for large-scale field campaigns (Stohl et al., 2004). Version 6.0 saw corrections to the numerics in the convection scheme, the addition of a domain-filling option used for instance in water-cycle studies (Stohl and James, 2004), and the possibility to use
30 nested output. Version 6.2, which added the ability to model sources and receptors in both mass and mixing ratio units (Seibert and Frank, 2004), is currently the last version described in a publication (Stohl et al., 2005). A separate sister model branch (v6.4) was adapted to run with NCEP GFS meteorological input data. The current paper describes the most important model developments that were done since v6.2 (for ECMWF) and v6.4 (for GFS).

Version 8.0 unified the model branches based on ECMWF-IFS and NCEP-GFS input data in one source package, but still required the building of two different executables. Importantly, Fortran 90 constructs were introduced in parts of the code, such as initial support of dynamic memory allocation. Furthermore, a global landuse inventory was added, allowing more accurate dry deposition calculations everywhere on the globe (before, landuse data were provided only for Europe). The

5   reading of the – at the time – newly introduced GRIB-2 format with ECMWF's grib_api library was implemented in v8.2. An option to calculate the sensitivity to initial conditions in backward model runs (in addition to the emission sensitivity calculations) was implemented also in v8.2. Version 8 was also the first version that distinguished between in-cloud and below-cloud scavenging for washout, relying on simple diagnostics for clouds based on grid-scale relative humidity. With a growing number of parameters defining removal processes, each species was given its own definition file, whereas in previous versions

10   the properties for all species were contained in a single file. The gravitational settling scheme was improved in v8.2.1 (Stohl et al., 2011), and this is briefly described in this paper in section 2.2.

For v9, the code was transformed to the Fortran 90 free-form source format. The option to read the run specifications from Fortran namelists instead of the standard input files was introduced, as described in section 5 of this paper. This change was motivated by the resulting greater flexibility, in particular with regard to setting of default values, optional arguments, when new

15   developments require adding new parameters, and when specifying parameter lists. In addition, an option to produce output in compressed NetCDF 4 format was provided (see section 6.3). Another option to write some model output only for the first vertical layer to save storage space for inverse modelling applications was also introduced (Thompson and Stohl, 2014) (see section 2.5).

1.3 FLEXPART version 10.3

20   For v10.3 of FLEXPART, described in this paper, several more changes and improvements were made. First, an optional new scheme applying more realistic skewed rather than Gaussian turbulence statistics in the convective atmospheric boundary layer (ABL) was developed (section 2.1). Second, the wet deposition scheme for aerosols was totally revised (Grythe et al., 2017), introducing dependencies on aerosol size, precipitation type (rain or snow) and distinguishing between in-cloud and below-cloud scavenging (see section 2.3). The code now also allows reading of three-dimensional (3-D) cloud water fields

25   from meteorological input files. Third, a method to calculate the sensitivity of deposited quantities to sources in backward mode was developed (section 2.4) Fourth, chemical reactions with the hydroxyl radical (OH) are now made dependent on the temperature and vary sub-monthly (section 2.6). Fifth, large parts of the code were parallelized using the Message Passing Interface (MPI), thus facilitating a substantial speed-up for certain applications (see section 3) and the code was unified so that a single executable can now use both ECMWF and GFS input data. Sixth, a dust mobilization scheme that can be run

30   as a FLEXPART pre-processor was developed (section 2.7). Seventh, the software used to retrieve data from ECMWF has been modernized and can now be used also by scientists from non-ECMWF member states (section 5.2.1). Finally, a testing environment was created that allows users to verify their FLEXPART installation and compare results (section 7).

Despite the many changes and additions, in large parts the operation of FLEXPART v10.3 still resembles the original version 1 design. Throughout this paper, we avoid repeating information on aspects of the model that have not changed since earlier

model descriptions. The paper should therefore always be considered together with the publications of Stohl et al. (1998, 2005). To provide the necessary context for the rest of this paper, we provide a brief overview of the FLEXPART v10.3 directory structure in Table 1. The source code is contained in directory `src`. The pathnames of the input and output directories are stated in the file `pathnames` read by the FLEXPART executable. The directory `options` contains the parameters that define

5   a run in files such as `COMMAND` (e.g. start/end times of the simulation, output frequency, etc.), `RELEASES` (definition of the particle releases), `OUTGRID` (output grid specifications) and others. All the output is written in a directory unique for each run. There are also other directories containing the model testing environment and example runs, and pre- and post-processing software (see Table 1).

Table 1. Directory structure overview of the FLEXPART v10.3 software distribution. All listed directories are subdirectories of the installation root directory `$flexhome/`.

	Subdirectory or file	Contents	Description/comments
`$flexhome/`	pathnames (file)	`$options/`	path to `options` directory
		`$output/`	path to `output` directory
		`$flex_winds/`	path to meteorological input files
		`$AVAILABLE`	path to `AVAILABLE` file
	src/	`*.f90`	Fortran source files
		`makefile`	see Section 4 and Appendix A
		`FLEXPART`	executable file (see Section 4)
	options/	COMMAND, RELEASES, OUTGRID, SPECIES, AGECLASSES, OUTGRID_NEST, RECEPTORS, IGBP_int1.dat , surfdata.t, surfdepo.t, OH_variables.bin	User input files see Section 5 and Table 5
	AVAILABLE	list of meteorological input data files	file containing list, see Section 5
	output/	FLEXPART output files	see Section 6 and Table 9
	preprocess/	`flex_extract/`	see Section 5.2
	postprocess/	`read_flex_fortran/`, `read_flex_matlab/`,	see Section 6.4
	tests/	development tests for FLEXPART and ancillary software	see Section 7
	tests/examples/	example runs illustrating various FLEXPART functionalities	and Appendix C

2   Updates of the model physics and chemistry

This section gives an overview over the main updates of the model physics and chemistry since the last published FLEXPART version, v6.2 (Stohl et al., 2005). Some developments have been published already separately, and in such cases we keep the description short, focussing on technical aspects of the implementation in FLEXPART that are important for the model users,

5   or demonstrating applications not covered in the original papers.

2.1   Boundary layer turbulence

Sub-grid scale atmospheric motions unresolved by the meteorological input data need to be parameterized in FLEXPART. This is done by adding stochastic fluctuations based on Langevin equations for the particle velocity components (Stohl et al., 2005). In the ABL, the stochastic differential equations are formulated according to the well-mixed criteria proposed by Thomson

10   (1987). Until FLEXPART version 9.2, the Eulerian probability density functions (PDFs) for the three velocity components were assumed to be three independent Gaussian PDFs. However, for the vertical velocity component, the Gaussian turbulence model is well suited only for stable and neutral conditions. In the convective ABL (CBL), turbulence is skewed since a larger area is occupied by downdrafts than by updrafts (e.g. Stull, 1988; Luhar and Britter, 1989). In such conditions, the Gaussian turbulence model is not appropriate for sources within the ABL, as it cannot reproduce the observed upward bending of plumes

15   from near-ground sources or the rapid downward transport of plumes from elevated sources (Venkatram and Wyngaard, 1988). However, the Gaussian approximation has negligible influence once the tracer is mixed throughout the whole ABL.

Cassiani et al. (2015) developed an alternative Langevin equation model for the vertical particle velocity including both skewed turbulence and a vertical density gradient, which is now implemented in FLEXPART v10.3. This scheme can be activated by setting the switch CBL to 1 in the file COMMAND. In this case, the time-step requirement for numerical stability

20   is much more stringent than for the standard Gaussian-turbulence model (typically, values of CTL=10 and IFINE=10 are required, also set in the file COMMAND). Therefore, considering that also the computation time required for each time step is about 2.5 times that of the standard Gaussian formulation, the CBL option is much more computationally demanding and not recommended for large-scale applications. However, for studies of tracer dispersion in the vicinity of individual point sources, the CBL option is essential to reproduce the characteristic features of CBL dispersion (Weil, 1985) while the additional

25   computational burden remains tolerable.

Figure 1 shows a comparison between two simulations of dispersion from an elevated source, with the skewed and with the Gaussian turbulence model. It can be seen that the maximum time-averaged ground-level concentration is about 30% higher for the skewed-turbulence parameterization. This is the result of the plume centre-line tilting downward to the surface in the vicinity of the source for the skewed-turbulence case, due to downdrafts being more frequent than updrafts. The plume also

30   spreads faster in this case. These results are similar to those obtained by others (e.g. Luhar and Britter, 1989).

It is important to note that the CBL formulation smoothly transits to a standard Gaussian formulation when the stability changes towards neutral (Cassiani et al., 2015). However, the actual equation solved inside the model for the Gaussian condition
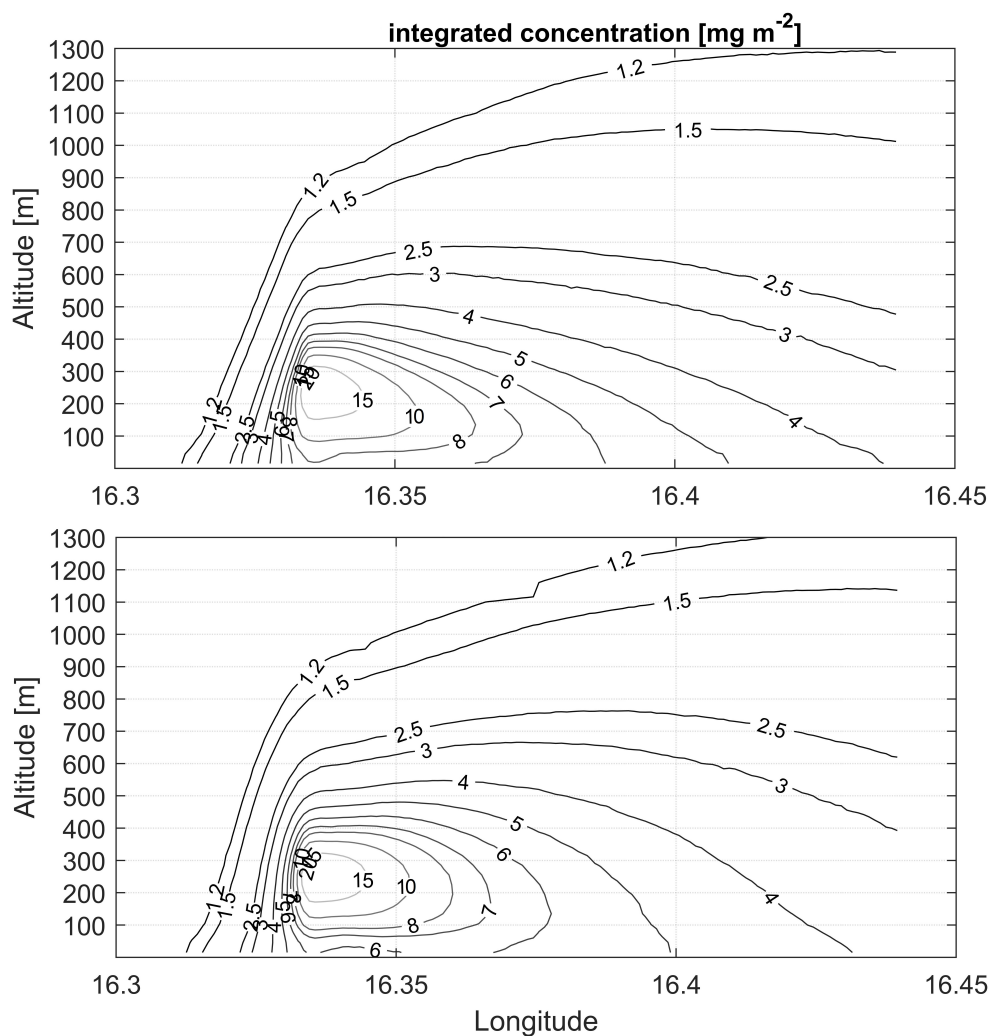
Figure 1. Comparison of FLEXPART results obtained with the skewed turbulence parameterization (upper panel) and with the Gaussian turbulence parameterization (lower panel). Shown are the tracer concentrations integrated over all latitudes as a function of altitude and longitude. The simulations used a point source emitting 100 kg of tracer per hour for a period starting on 1 July 2017 at 12:00 UTC. The source was located at 47.9157°E and 16.3274° N, 250 m above ground level. Results are averaged for the time period 12:40 to 13:00 UTC. The reader should note that the maximum ground level concentration in the upper panel is about 30% higher than in the lower panel.

is still different from the standard version as actual particle velocities rather than the scaled ones are advanced (see, e.g. Wilson et al., 1981; Rodean, 1996). Full details of the CBL implementation can be found in Cassiani et al. (2015).

To date, FLEXPART has mainly been used for large-scale applications. With this new CBL option, FLEXPART is now also well suited for the simulation of small-scale tracer dispersion, or for inverse modelling of point-source emissions from

5 near-field measurements – at least if the resolved winds are representative of the situation considered. In fact, to our knowledge FLEXPART is the only particle model considering both skewness in the vertical velocity distribution and vertical gradients in air density. Both these effects are particularly important in deep CBLs and can be additive with respect to simulated ground-level concentrations.

2.2 Gravitational settling

10 Gravitational settling of aerosols is implemented in FLEXPART as a process that changes the particle trajectories. The settling velocity is determined at each time step and added to the vertical wind velocity. In simulations where a particle represents several species, all species are transported with the settling velocity of the first species. If this is undesired, simulations for the different species must be run separately. Gravitational settling velocities are also used in the calculation of dry deposition.

In older FLEXPART versions, gravitational settling was calculated using a single dynamic viscosity of air. With FLEXPART

15 8.2.1, the gravitational settling calculation was generalized to higher Reynolds numbers and it takes into account the temperature dependence of dynamic viscosity. This is done in subroutine get_settling.f90 in an iterative loop, where both the Reynolds number and the settling velocity are determined (Naeslund and Thaning, 1991). For initialization of the loop, Stokes' law and a constant-viscosity estimate is used. The dynamic viscosity is calculated as a function of temperature using the formula of Sutherland (1893). Spherical shape of the particles is assumed in the settling calculation, which could be further

20 extended in the future to allow for more complex particle shapes. For particle sizes of about 10 μm, settling velocities in the new FLEXPART version are not much different from earlier versions using the old settling calculation, typically by less than 20%. However, differences are largest in the cold upper troposphere, implying, for instance, changes in the residence time of volcanic ash particles at heights relevant for aviation.

2.3 Wet deposition

25 In FLEXPART, the calculation of wet scavenging is divided into three parts: First, it is determined where scavenging occurs and which form it takes (e.g. below- or within-cloud scavenging). Second, the scavenging coefficient is determined and, third, the actual removal of particle mass is calculated.

With respect to the first part, it is important to understand that wet scavenging occurs only in the presence of clouds and where precipitation occurs. In air columns without clouds, above the top of the clouds, and where the total precipitation rate I_t (the

30 sum of large scale and convective precipitation) does not exceed 0.01 mm h^{-1}, no scavenging occurs.To quickly know where a particle is located relative to the clouds, in subroutines verttransform_ecmwf.f90 or verttransform_gfs.f90 each grid cell is categorised as being either in a cloud-free column, above a cloud, inside a cloud, or below a cloud. This cloud definition has been revised completely compared to earlier versions and is described in section 2.3.1.

With respect to the second step, the scavenging coefficient Λ (s^{-1}) is determined in subroutine `get_wetscav.f90`. After a series of updates, in particular Grythe et al. (2017), FLEXPART now distinguishes between below-cloud and in-cloud scavenging and has also different parameterizations of Λ for gases and particles. For the latter, it also distinguishes between liquid-phase and ice-phase states. This yields in total six different parameterizations for Λ, described in sections 2.3.2 and

5 2.3.3.

In the third step, the removal of particle mass due to wet deposition is calculated. It takes the form of an exponential decay process (McMahon, 1979),

$$m(t + \Delta t) = m(t) \exp(-\Lambda \Delta t) , \tag{1}$$

where m is the particle mass (kg) (it can also be a mass mixing ratio, depending on settings in file `COMMAND`). This removal

10 of particle mass and corresponding accumulation of deposition at the surface is calculated in subroutine `wetdepo.f90` and has not been changed since earlier versions.

2.3.1 Definition of clouds, cloud water content and precipitation

The location of clouds, the total cloud column water content and phase, and precipitation intensity and phase are needed in the calculation of the wet scavenging. Therefore, a three-dimensional cloud mask is defined in subroutine `verttransform_ecmwf.f90`

15 (or `verttransform_gfs.f90` for GFS data). In previous FLEXPART versions, the cloud definition scheme was very simple and based on relative humidity (RH). In grid columns with precipitation, grid cells with RH>80% were defined as in-cloud, and those with RH<80% were set as below-cloud up to the bottom of the uppermost layer with RH>80%. This was appropriate for the first version of FLEXPART, as ECMWF had a similarly simple definition of clouds and more detailed information was not available from the ECMWF archives at the time.

20 If no cloud information is available from the meteorological data, the old RH-based scheme is still used in FLEXPART. However, nowadays, specific cloud liquid water content (CLWC, [kg kg^{-1}]) and specific cloud ice water content (CIWC, [kg kg^{-1}]) are available as 3-D fields in meteorological analyses from ECMWF, and also NCEP provides the 3-D cloud water mixing ratio ($CLWMR$, [kg kg^{-1}]), furtheron referred to as q_c. A cloudy grid cell is defined when $q_c > 0$. FLEXPART v10.3 can ingest the ECMWF CLWC and CIWC either separately, or as the sum ($q_c = CLWC + CIWC$). However, to save storage

25 space, we recommend to retrieve only the sum, q_c, from ECMWF, as the relative fractions of ice and liquid water can be parameterized quite accurately using equation 4.

The column cloud water (c_l) [kg m^{-2}], which is needed for the in-cloud scavenging parameterization, is calculated by integrating q_c over all vertical z levels

$$c_l = \sum_z q_c(z) \rho_{air}(z) \Delta z , \tag{2}$$

30 where $\rho_{air}(z)$ is the density of the air in the grid cell, and Δz is the vertical extent of the grid cell. In older FLEXPART versions, c_l was parameterized based on an empirical equation given in Hertel et al. (1995), using the sub-grid (see below, how sub-grid is defined) surface precipitation rate I_s [mm/h]. While such a parameterization is not needed anymore if q_c is available,

it is still activated in case cloud water input data are missing. However, in order to ensure that c_l from the parameterization is statistically consistent with the cloud data, we derived the modified expression

$$c_l = 0.5 \times I_s^{0.36} \, , \tag{3}$$

using a regression analysis between existing cloud and precipitation data.

5   Precipitation is not uniform within a grid cell. To account for sub-grid variability, it is assumed that precipitation is enhanced within a sub-grid area, and that no precipitation (and thus no scavenging) occurs outside this sub-grid area. The sub-grid area fraction and precipitation rate (I_s) are estimated from the grid-scale precipitation rate (I_t), based on values tabulated in Hertel et al. (1995). It is used for all scavenging processes in FLEXPART, and maintained from previous FLEXPART versions as described in Stohl et al. (2005).

10   The precipitation phase needed for the below-cloud scavenging scheme is simply based on ambient grid-scale temperature, with snow occurring below $0°C$ and rain above. For cloud water, c_l, we assume a temperature-dependent mixture of liquid and solid particles, where the liquid fraction (α) is calculated based on the local temperature T,

$$\alpha = \left(\frac{T - T_L}{T_L - T_I} \right)^2 \, , \tag{4}$$

where $T_L = 0°C$ and $T_I = -20°C$. For $T > T_L$, $\alpha = 1$ and for $T < T_I$, $\alpha = 0$. Even when CLWC and CIWC are available
15   as separate fields, we derive the liquid fraction (α) of cloud water from the local temperature. Comparisons have shown that CLWC is very accurately reproduced by $\alpha \times q_c$.

The cloud information should be linearly interpolated like the other variables, and situations where the diagnosed cloud is incompatible with the precipitation rate (be it because of interpolation, or because of convective precipitation accompanied by too shallow or lacking grid-scale clouds) need to receive special treatment. This is planned for a version upgrade in the
20   near future, in conjunction with a better interpolation scheme for precipitation (see Hittmeir et al., 2018). In certain cases, the deposition calculation of FLEXPART might be improved by using higher-resolution precipitation data from other sources such as, for example, from radar observations (Arnold et al., 2015); however, as then precipitation and ECMWF cloud data may not match, this does not guarantee better results.

2.3.2   Below cloud scavenging

25   For gases, the scavenging coefficient, Λ, for below-cloud scavenging is calculated as described in Asman (1995),

$$\Lambda = A I_s^B \, , \tag{5}$$

where the scavenging parameters A and B depend on the chemical properties of the gas and are specified in the `SPECIES_nnn` file as described in Appendix 5.1.3 (`nnn` represents the species number (0-999) used for the simulation). In older FLEXPART versions, this scheme was used also for aerosols; however, Grythe et al. (2017) developed a new aerosol scavenging scheme
30   that is implemented in FLEXPART v10.3 and briefly summarized here.

The relevant processes of collision and attachment of ambient aerosol particles to falling precipitation depend mainly on the relationship between the aerosol and hydrometeor size and type (rain or snow) and to a lesser degree on the density and hygroscopicity of the aerosol. In FLEXPART v10.3, the dependence of scavenging on the sizes of both the aerosol and falling hydrometeors are taken into account by the schemes of Laakso et al. (2003) for rain and Kyrö et al. (2009) for snow. Both

5 schemes follow the equation

$$log_{10}(\frac{\Lambda}{\Lambda_0}) = C_*(a + b\,D_p^{-4} + c\,D_p^{-3} + d\,D_p^{-2} + e\,D_p^{-1} + f(\frac{I_s}{I_0})^{0.5}) ,\qquad(6)$$

where $D_p = log_{10}\frac{d_p}{d_{p0}}$, d_p is the particle dry diameter provided in the SPECIES_nnn file, $d_{p0} = 1\,\mathrm{m}$, $\Lambda_0 = 1\,\mathrm{s^{-1}}$, and $I_0 = 1\,\mathrm{mm\,h^{-1}}$. Coefficients for factors $a - f$ are different for rain and snow scavenging and are given in Table 2. The C_* values are collection efficiencies that reflect the properties of the aerosol and must be given for both rain ($C_* = C_{\mathrm{rain}}$) and snow

10 scavenging ($C_* = C_{\mathrm{snow}}$) in the SPECIES_nnn file. Notice that by setting $C_{\mathrm{snow}} = 0$, below cloud scavenging by snowfall is switched off (similarly, $C_{\mathrm{rain}} = 0$ for rain).

Table 2. Parameters used in Eq. 6 for below cloud scavenging.

	C_*	a	b	c	d	e	f	Reference
Rain scavenging	C_{rain}	274.36	332839.6	226656	58005.9	6588.38	0.24498	Laakso et al. (2003)
Snow scavenging	C_{snow}	22.7	0	0	1321	381	0	Kyrö et al. (2009)

2.3.3 In-cloud scavenging

For in-cloud scavenging of both aerosols and gases, Λ is calculated as described in Grythe et al. (2017):

$$\Lambda = ic_r S_i I_s ,\qquad(7)$$

15 where $ic_r = 6.2$ is the cloud water replenishment factor, which was determined empirically in Grythe et al. (2017), and S_i is proportional to the in-cloud scavenging ratio, which is derived differently for gases and aerosols.

For gases, $S_i = \frac{1}{\frac{1-cl}{HRT} + cl}$, where H is Henry's constant (describing the solubility of the gas and specified in the SPECIES_nnn file), R is the gas constant, and T is temperature. Notice that this is applied for both liquid phase and ice clouds.

For aerosols, the in-cloud scavenging is dominated by activated particles forming cloud droplets or ice nuclei. Those may

20 eventually combine to form a hydrometeor which falls out of the cloud, thus removing all aerosol particles contained in it. Therefore, S_i depends on the nucleation efficiency (F_{nuc}) and cl:

$$S_i = \frac{F_{\mathrm{nuc}}}{cl} .\qquad(8)$$

F_{nuc} describes how efficiently the aerosol particles are activated as cloud droplet condensation nuclei (CCN) or ice nuclei (IN):

25 $$F_{\mathrm{nuc}} = (1 - \alpha)CCN_{\mathrm{eff}} + \alpha IN_{\mathrm{eff}} ,\qquad(9)$$

where the relative abundances of the liquid and ice phase are accounted for by the factor α. Values for the efficiencies, CCN_{eff} and IN_{eff}, are available from the literature for many different types of aerosols (e. g. black carbon, mineral dust particles, or soluble particles) and some have been collected in `SPECIES_nnn` files distributed with FLEXPART (see appendix 5.1.3). The CCN_{eff} and IN_{eff} values are set for an aerodynamic particle radius of 1 μm but CCN and IN efficiencies increase with increasing

5   particle size. The in-cloud parameterization takes this into account. For further details on the wet scavenging scheme used in FLEXPART, see Grythe et al. (2017).

2.3.4   Influence of wet scavenging on the aerosol lifetime

Aerosol wet scavenging controls the lifetime of most aerosols. In Fig. 2, we compare modelled e-folding lifetimes from a number of FLEXPART simulations, using different model versions, and switching off in-cloud and below-cloud scavenging

10   in FLEXPART v10.3 with measured lifetimes. The parameter settings in FLEXPART used for these comparisons were the same as used by Grythe et al. (2017). To derive aerosol lifetimes in a consistent way from both measurements and model simulations, a radionuclide attached to ambient aerosol and a noble-gas radionuclide were used. Kristiansen et al. (2016) used the same method to compare many different aerosol models, and we refer to their paper for more details on the method. For our model simulations, several size bins of aerosols were used, though total concentrations and lifetimes are largely controlled by

15   0.4 and 0.6 μm particles (see Grythe et al., 2017). E-folding lifetimes increase from 5.8 to 10.0 days between FLEXPART v9 and v10.3. A simulation performed with v10.3 but which emulated the in-cloud scavenging of v9 showed that the difference is mainly due to the decreased in-cloud scavenging in the new removal scheme compared to the old one. Notice that the lifetime obtained with v10.3 is much closer to the observation-based lifetimes. Turning off the below-cloud removal has a relatively small effect, increasing the lifetime to 11 days, whereas turning off the in-cloud removal extends the lifetime to the unrealistic

20   value of 66 days (see bottom two panels in Fig. 2). This highlights the dominant role of in-cloud removal for accumulation mode particles in FLEXPART.

Notice that, compared to older versions of FLEXPART, the `SPECIES_nnn` files now include additional parameters related to the wet deposition scheme. Old input files, therefore, need to be updated for use with FLEXPART v10.3. The required format changes are detailed in Appendix 5.1.3.

25   2.4   Source-receptor matrix calculation of deposited mass backward in time

When running FLEXPART forward in time for a depositing species with a given emission flux (kg per release as specified in file `RELEASES`), the accumulated wet and dry deposition fluxes in units of ng/m^2 are appended to the FLEXPART output files (`grid_conc_date` and/or `grid_pptv_date`, where `date` represents the date and time in format `YYYYMMDDhhmmss`, see section 6) containing the atmospheric concentration and/or volume mixing ratio output. The deposition is always given in

30   mass units, even if atmospheric values are given in mixing ratio units. In contrast to concentration values, deposition quantities are accumulated over the time of the simulation, so the deposited quantities generally increase during a simulation (except when radioactive decay is activated, which also affects deposited quantities and can decrease them).
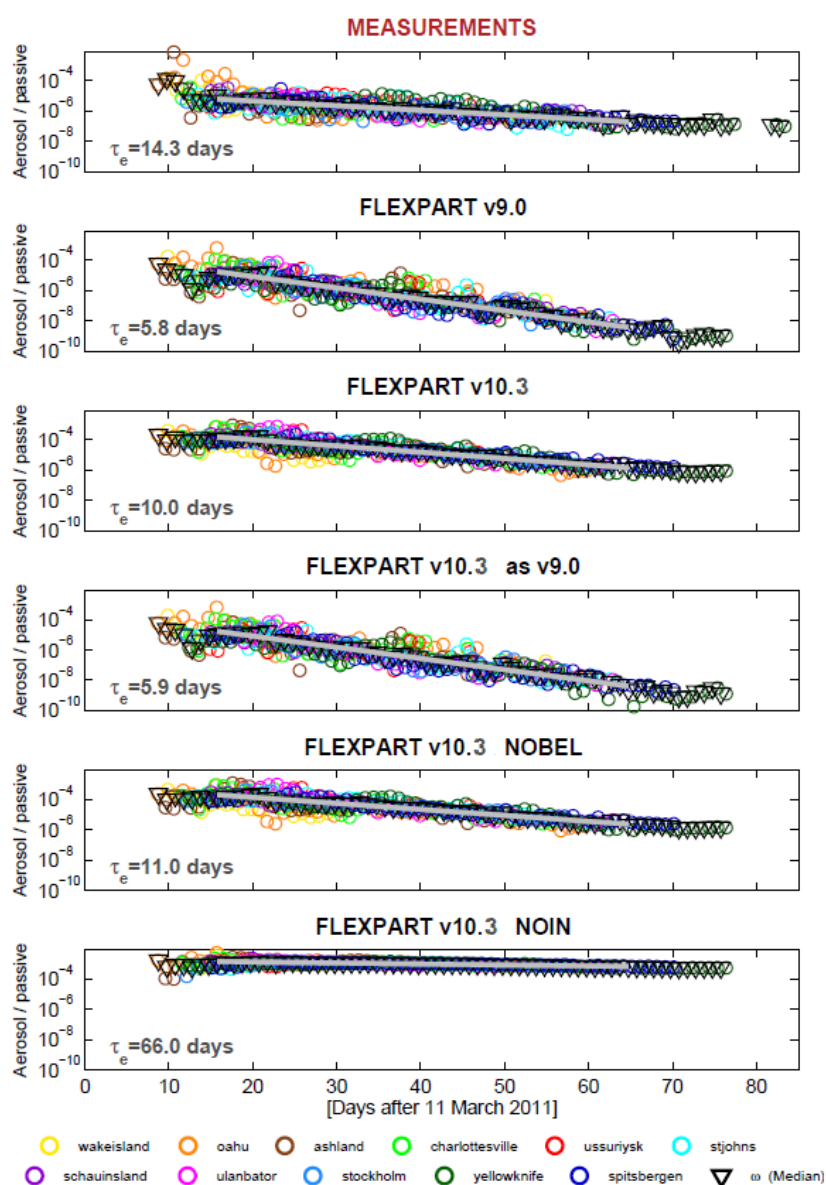
Figure 2. Aerosol lifetimes estimated from the decrease of radionuclide ratios (aerosol-bound ^{137}Cs and noble gas ^{133}Xe as a passive tracer) with time after the Fukushima nuclear accident, as measured and modelled at a number of global measurement stations. For details on the method, see Kristiansen et al. (2016). E-folding lifetimes, τ_e, are estimated based on fits to the data and reported in each panel. In the top panel, the observed values are shown and in subsequent panels from the top, modelled values are given for FLEXPART v9, FLEXPART v10.3, FLEXPART v10.3 with parameter settings to emulate removal as in v9, FLEXPART v10.3 with no below-cloud removal and FLEXPART v10.3 with no in-cloud removal.

As discussed in Section 1, running FLEXPART backward in time for calculating SRRs is more efficient than running it forward if the number of (potential) sources is larger than the number of receptors. For atmospheric concentrations (or mixing ratios), the backward mode has been available from the very beginning, and in an improved form since FLEXPART v5 (Stohl et al., 2003; Seibert and Frank, 2004). This has proved very useful for the interpretation of ground-based, ship-borne or air-borne

5 observations (e.g. to characterize sources contributing to pollution plumes). Furthermore, the inversion scheme FLEXINVERT (Thompson and Stohl, 2014) that is used to determine the fluxes of greenhouse gases is based on backward simulations. However, there also exist measurements of deposition on the ground, e.g. in precipitation samples or ice cores, and for this type of measurements no backward simulations were possible until recently. Therefore, Eckhardt et al. (2017) introduced the option to calculate SRR values in backward mode also for wet and dry deposition, and a first application to ice core data was presented

10 by McConnell et al. (2018). It is anticipated that quantitative interpretation of ice core data will be a major application of the new backward mode, which is efficient enough to allow calculation of, say 100 years of seasonally resolved deposition data in less than 24 hours of computation time.

We illustrate the different backward modes and explain the required settings at the example of calculations for a single receptor location, Ny Ålesund in Spitsbergen (78.93°N, 11.92°E) and for the 24-hour period from 18 August 2013 at 20 UTC

15 to 19 August 2013 at 20 UTC. SRR values are calculated for the atmospheric concentration averaged over the layer $0-100$ m agl, as well as for wet and dry deposition. The substance transported is black carbon (BC) which is subject to both dry and wet deposition. Backward simulations for wet and dry deposition must always be run separately. In order to obtain SRR values for total deposition, results for wet and dry deposition need to be summed.

The backward mode is activated by setting the simulation direction, LDIRECT in file COMMAND (see section 5), to –1. The

20 three simulations are obtained by consecutively setting IND_RECEPTOR to 1 (for concentration), 3 (wet deposition) and 4 (dry deposition), respectively. IND_SOURCE is always set to 1, meaning that the sensitivities (SRR values) are calculated with respect to physical emissions in mass units. A complete list of possible options is reported in Table 1 of Eckhardt et al. (2017).

Figure 3 shows the resulting SRR (i.e. emission sensitivity) fields for the concentration, dry and wet deposition at the receptor. Dry deposition occurs on the Earth's surface, therefore particles are released in a shallow layer adjacent to the surface.

25 Its height is consistent with the shallow depth over which dry deposition is calculated in forward mode (user settings for the release height are ignored for dry deposition backward calculations). Dry deposition rates are the product of the surface concentration and the deposition velocity. Therefore, the SRR fields for surface concentration (Fig. 3a) and dry deposition (Fig. 3b) show similar patterns, in this case indicating high sensitivity for sources over Scandinavia and northwestern Russia. The differences in the spatial patterns are mainly due to temporal variability in the dry deposition velocity at the receptor

30 caused by varying meteorological conditions (e.g. stability) and surface conditions during the 24-hour release interval.

Wet deposition, on the other hand, can occur anywhere in the atmospheric column from the surface to the top of the precipitating cloud. FLEXPART automatically releases particles in the whole atmospheric column (again, user settings for the release height are ignored), but particles for which no scavenging occurs (e.g. those above the cloud top, or when no precipitation occurs) are immediately terminated. Therefore, and because of vertical variability of the scavenging process, the sensitivity

35 for the deposited mass can deviate significantly from the sensitivity corresponding to surface concentration. Here (Fig. 3c),
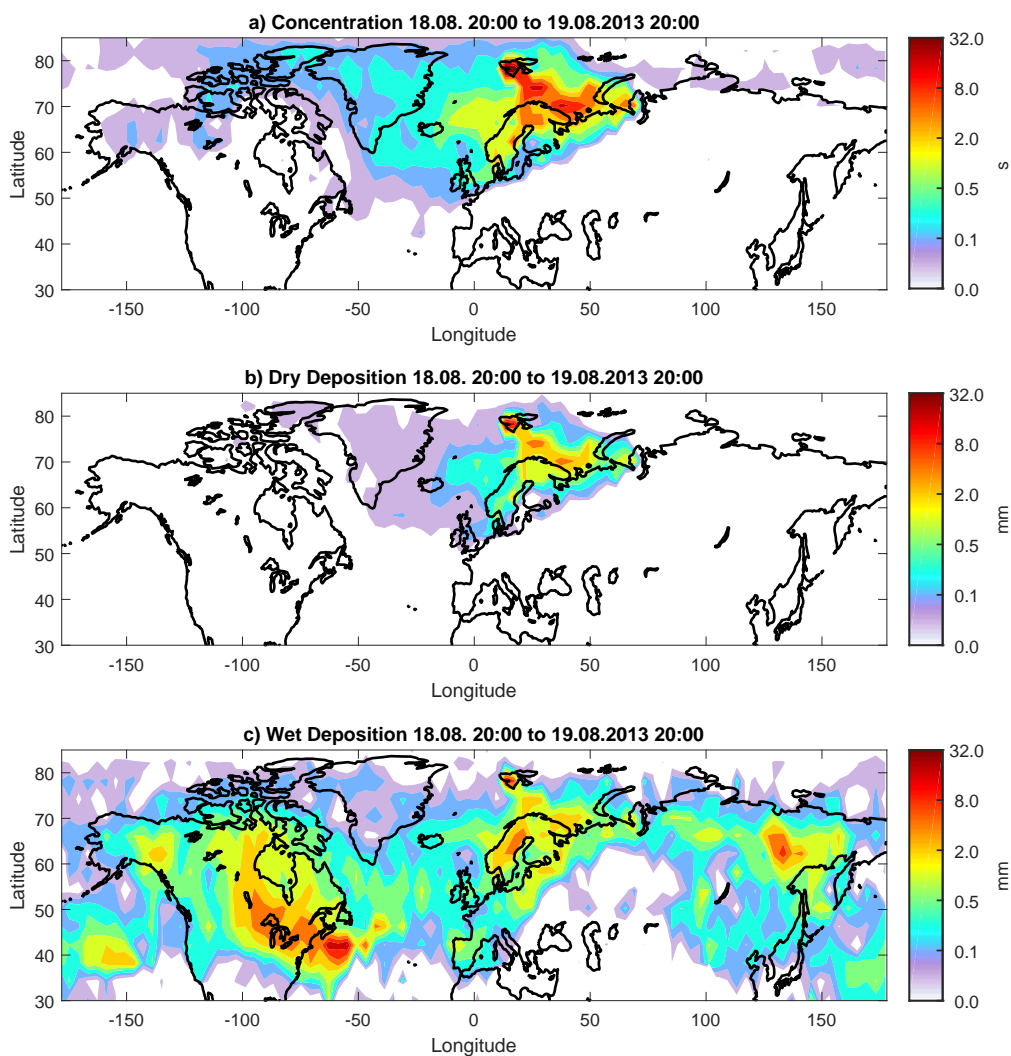
Figure 3. Source-receptor relationships (for emissions occurring in the lowest 100 m a.g.l.) for black carbon observed at Ny Ålesund in Svalbard for a 24-hour period starting on 18 August 2013 at 20 UTC. The sensitivities were calculated for (a) concentrations (s) in the layer 0 – 100 m agl, (b) dry deposition (mm), and (c) wet deposition (mm).**19**

the sensitivity is high over Scandinavia and northwestern Russia, as was already seen for surface air concentrations and dry deposition. However, in addition, sources located in North America and Eastern Siberia also contribute strongly to the wet deposition. The maximum over the ocean close to the North American east coast is likely due to lifting in a warm conveyor belt, followed by fast transport at high altitude.

5   Concentration, dry deposition and wet deposition at the receptor can be calculated from the SRR fields shown in Fig. 3 as follows:

$$c = \boldsymbol{m}_c \cdot \boldsymbol{q}$$
$$d_d = \boldsymbol{m}_d \cdot \boldsymbol{q}$$
$$d_w = \boldsymbol{m}_w \cdot \boldsymbol{q}$$

(10)

Here, c is the modelled concentration (in $\mathrm{kg\,m^{-3}}$), d_d the dry deposition rate, and d_w the wet deposition rate (both in $\mathrm{kg\,m^{-2}\,s^{-1}}$). In this specific case with only a single, scalar receptor, the source-receptor matrix degenerates to a vector of

10   the SRR values, one for each of the three types of receptors ($\boldsymbol{m}_c$ for concentration in units of s, $\boldsymbol{m}_d$ for dry deposition and $\boldsymbol{m}_w$ for wet deposition, both in units of m). In order to obtain the concentration or the deposition rates, these vectors need to be multiplied with the vector of emissions $\boldsymbol{q}$ (in $\mathrm{kg\,m^{-3}\,s^{-1}}$). If the total deposition is desired, the deposition rates d_d and d_w can be multiplied with the receptor time interval ΔT_r, in our case 86400 s (24 h). Note that this is the period during which particles are released according to the specification of the RELEASES file. The emission fluxes must be volume averages over

15   the output grid cells specified in the OUTGRID file, typically surface emission fluxes (in $\mathrm{kg\,m^{-2}\,s^{-1}}$) divided by the height of the lowermost model layer.

2.5   Sensitivity to initial conditions

Backward simulations with FLEXPART in the context of inverse modelling problems typically track particles for several days up to a few weeks. This is sufficient to estimate concentrations at the receptor only for species with atmospheric lifetimes

20   shorter than this period. Many important species (e.g. greenhouse gases such as methane) have considerably longer lifetimes. For such long-lived species, most of the atmospheric concentration variability is still caused by emission and loss processes occurring within the last few days before a measurement because the impact of processes occurring at earlier times is smoothed out by atmospheric mixing. This leads to a relatively smooth "background" (in time series analyses sometimes also called a baseline) that often is a dominant fraction of the total concentration but that does not vary much with time, and short-term

25   fluctuations on top of it. The signal of the regional emissions around the measurement site is mostly contained in the short-term concentration fluctuations but in order to use it in inverse modelling, the background still needs to be accounted for, as otherwise no direct comparison to measurements is possible.

One simple method is to estimate the background from the measurements as, e. g. in Stohl et al. (2009). A better approach is to use a concentration field taken from a long-term forward simulation with a Eulerian model or with FLEXPART itself,

30   especially if nudged to observations (Groot Zwaaftink et al., 2018) as an initial condition for the backward simulation. This field needs to be interfaced with the FLEXPART backward simulation by calculating the receptor sensitivity to the initial conditions

Seibert and Frank (cf. Eqs. 2–6 in 2004). For a, say, 10-day backward simulation, the concentration field needs to be sampled at those points in time and space when and where each particle trajectory terminates 10 days back in time. Furthermore, it is necessary to quantify the effects of deposition or chemical loss during the backward simulation on this background (the factor $p(0)$ in Seibert and Frank (2004)). For example, chemical reactions with hydroxyl radicals will reduce initial concentrations of

5 methane en route to the receptor, even though not much during a 10-day period.

Since version 8.2, FLEXPART provides an option for quantifying the influence of initial conditions on the receptor in backward simulations which is activated with the switch `LINIT_COND` in file `COMMAND`. Then, gridded fields containing the sensitivities to background mixing ratios (or concentrations, depending on user settings for the switch `LINIT_COND` in file `COMMAND`) are produced and stored in the output files `grid_initial_nnn` (where `nnn` stands for the species number),

10 on the same 3D grid as the regular output, defined in the files `OUTGRID` and `OUTGRID_NEST`. In this case, a concentration would be calculated as

$$c = \boldsymbol{m}_i \cdot \boldsymbol{c}_b + \boldsymbol{m}_c \cdot \boldsymbol{q} \tag{11}$$

where $\boldsymbol{m}_i$ denotes the sensitivity to the initial condition and $\boldsymbol{c}_b$ the background concentration when and where particles are terminated.

15 Figure 4 shows an example of the use of the sensitivities of receptor mixing ratios (here, of methane) both to surface emissions and initial conditions. The top right panel shows the sensitivity to surface emissions on one particular day, the lower two panels show the sensitivity to initial conditions below and above 3000 m for the same day. Both results are from a 8-day backward simulation from one receptor site in Sweden. It can be seen that the sensitivity to emissions is highest close to the station but there is also substantial sensitivity to emission uptake over large parts of Central and Eastern Europe. The particles

20 terminated 8 days before arrival at the receptor in a roughly croissant-shaped area covering large parts of Europe and the North Atlantic, as indicated by the sensitivity to initial conditions. Most of the sensitivity is located below 3000 m but there is also some influence from higher levels. Notice that only two layers are shown in Fig. 4, whereas the real model output has much higher vertical resolution.

The sensitivity to initial conditions was interfaced with a domain-filling methane forward simulation as described in (Groot

25 Zwaaftink et al., 2018) (not shown), while the emission sensitivity was interfaced with an emission inventory for methane (not shown), as given by equation 11. This was done for daily simulations throughout one month, thus generating a time series of background mixing ratios (from the first term in equation 11 only), and total mixing ratios (top left panel in Fig. 4). The latter include the contributions from emissions during the 8-day backward simulation. It can be seen that the methane background advected from 8 days back varies relatively little between about 1910 and 1940 ppbv, while the emission contributions vary

30 from 0 (on 29 October) to about 200 ppbv (on 19 October, the date for which the sensitivity plots are shown).

In practical applications for inverse modelling, source-receptor sensitivities are often only needed at the surface (as most emissions occur there), while sensitivities to the background are needed in 3-D. By setting the option `SURF_ONLY` to 1 in the `COMMAND` file, the regular output files `grid_time_date_nnn` containing the source-receptor sensitivities will include only the first vertical level as defined in the file `OUTGRID`, while the full vertical resolution is retained in `grid_initial_nnn`
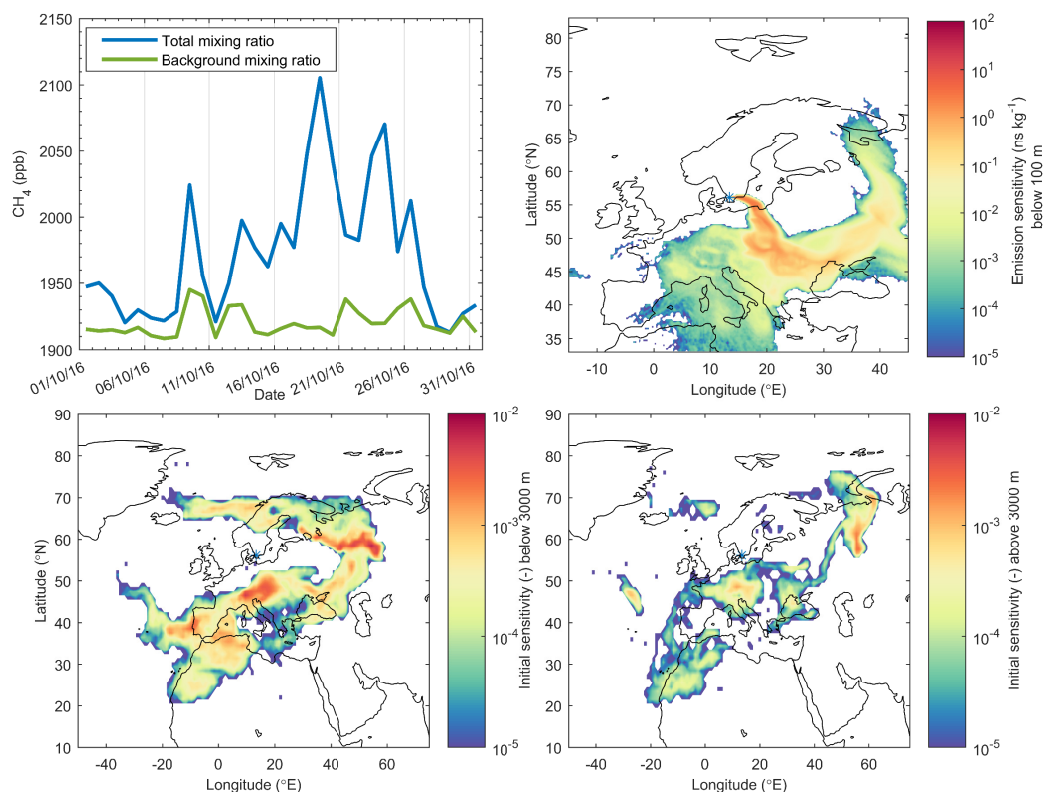
Figure 4. Example of FLEXPART 8-day backward runs for methane from a site in Southern Sweden (Hyltemossa) demonstrating the combined use of sensitivities to emissions and initial conditions. Top left: time series of methane background mixing ratios and total mixing ratios in October 2016. Top right: sensitivity of methane mixing ratio at Hyltemossa on 19 October 2016 to methane emissions at the surface. Lower left: sensitivity of methane mixing ratio at Hyltemossa on 19 October 2016 to methane initial conditions below 3000 m. Lower right: sensitivity of methane mixing ratio at Hyltemossa on 19 October 2016 to methane initial conditions above 3000 m. Blue asterisks on the maps mark the receptor location.

files containing the sensitivities to the initial conditions. Since the data amounts stored in the `grid_time_date_nnn` files can be much larger than in the `grid_initial_nnn` files, this is a highly efficient way to save storage space. This setup also interfaces directly with the inverse modelling package FLEXINVERT (Thompson and Stohl, 2014). An application can be found in Thompson et al. (2017) where initial conditions were taken from a gridded observation product.

2.6 Chemical reactions with the hydroxyl radical (OH)

The hydroxyl (OH) radical reacts with many gases and is the main cleansing agent in the atmosphere. While it is involved in highly non-linear atmospheric chemistry, for many substances (e.g. methane) a simplified linear treatment of loss by OH is possible, using prescribed OH fields. For this, monthly averaged $3° \times 5°$ resolution OH fields for 17 atmospheric layers are used in FLEXPART. The fields were obtained from simulations with the GEOS-CHEM model (Bey et al., 2001) and are read from the file `OH_variables.bin` by the subroutine `readOHfield.f90`.

Tracer mass is lost by reaction with OH if a positive value for the OH reaction rate is given in the file `SPECIES_nnn`. In FLEXPART v10.3, the OH reaction scheme was modified to account for (i) hourly variations in OH, and (ii) the temperature dependence of the OH reaction rate (Thompson et al., 2015). This makes the chemical loss calculations more accurate, especially for substances with shorter lifetimes (order of weeks to months), for example ethane. Hourly OH fields are calculated from the stored monthly fields by correcting them with the photolysis rate of ozone calculated with a simple parameterization for cloud-free conditions based on the solar zenith angle (`gethourlyOH.f90`):

$$OH = \frac{j}{j^*} OH^* \tag{12}$$

where j are the hourly photolysis rates calculated for all 3D locations in the field, while j^* are the corresponding monthly mean rates, pre-calculated and stored in file `OH_variables.bin` together with the monthly-mean fields OH^* (see section 5.1.8). The motivation for this is that OH production follows closely the production of $O(^1D)$ by photolysis of ozone, allowing this simple parameterization of OH variability. At any time, two hourly OH fields are in memory and are interpolated to the current time step. Figure 5 shows the annual and daily variation of OH for two locations as obtained with this simple parameterization.

The OH reaction rate κ (unit s^{-1}) is calculated in `ohreaction.f90` using the temperature-dependent formulation

$$\kappa = C T^N e^{-D/T} [OH] \tag{13}$$

where C, N and D are species-specific constants (assigned in the `SPECIES_nnn` files), T is the absolute temperature and $[OH]$ the OH concentration (Atkinson, 1997). As the OH concentration in file `OH_variables.bin` is given in units of molecules per cubic centimeter, the unit of C needs to be in cm^3 molecule^{-1} s^{-1}. The mass m of a given species after reaction with OH is determined as

$$m(t + \Delta t') = m(t) e^{-\kappa \Delta t'} \tag{14}$$

where $\Delta t'$ is the reaction time step (given by `lsynctime`).
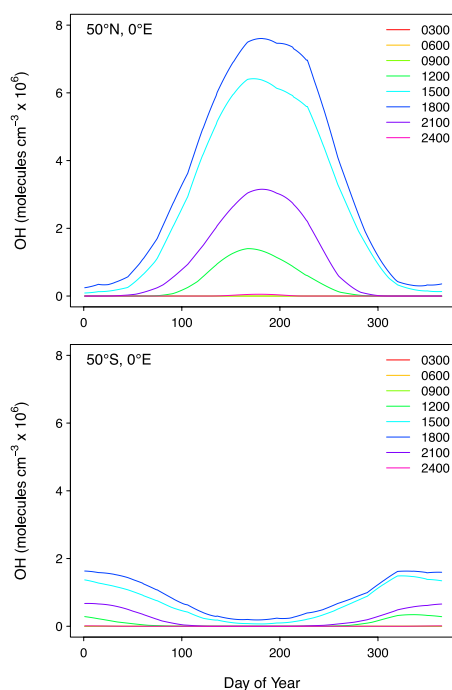
Figure 5. Annual and daily OH concentration variation as obtained with the simple parameterization based on photolysis rates of ozone for two locations, one in the Northern Hemisphere (top panel) and one in the Southern Hemisphere (bottom panel). Line labels correspond to the time of day.

Backwards compatibility with the former temperature-independent specification of the OH reaction (version 9 and before) can be achieved by setting the constant N in the `SPECIES_nnn` file to zero. The constants C and D can be derived from the former parameters as follows:

$$C = \kappa_r \, e^{D/T_r} \tag{15}$$

5   and

$$D = A/R \tag{16}$$

where A is the activation energy and R is the gas constant, and κ_r is the former OH reaction rate (referring to $T_r = 298\,\mathrm{K}$), which were specified in the `SPECIES_nnn` file for earlier versions.

Other OH fields than those provided with the model code have been tested in FLEXPART. These fields may have higher spatial and temporal resolution (e.g. Fang et al., 2016), important for chemical species with short lifetimes. Users are required to modify `readOHfield.f90` and `gethourlyOH.f90` to read in other OH fields, and be aware that expressions of OH reaction rate or reaction with OH might differ from those in the above equations. If this is the case users need to modify

5 `ohreaction.f90`, too.

2.7 Dust mobilisation scheme

Desert dust is a key natural aerosol with relevance for both climate and air quality. FLEXPART has been used earlier with preprocessors to initialize dust amounts from wind speed and surface properties following Tegen and Fung (1994) (Sodemann et al., 2015). Now a dust mobilisation routine has been included as a preprocessing tool in FLEXPART v10.3. The scheme

10 called FLEXDUST was developed to simulate mineral dust transport with FLEXPART in forward or backward simulations (Groot Zwaaftink et al., 2016). This module runs independently from FLEXPART and produces gridded output of mineral dust emission as well as input files (`RELEASES`) that can be used for FLEXPART simulations of atmospheric transport. It can thus be considered a preprocessing (for forward simulations) or postprocessing tool (for backward simulations) for FLEXPART v10.3.

15 In FLEXDUST, emission rates are estimated according to the emission scheme proposed by Marticorena and Bergametti (1995). We thereby assume that sandblasting occurs in case sand is present and a minimum threshold based on the size-dependent threshold friction velocity following Shao and Lu (2000) can be applied. ECMWF operational analysis or ERA Interim re-analysis data, the Global Land Cover by National Mapping Organizations version 2 (Tateishi et al., 2014) and sand and clay fractions from the Global Soil Data Task (2014) are used as input for the model. Erodibility is enhanced in topographic

20 depressions and dust emission is modified by soil moisture and snow cover. The module includes high-latitude dust sources in the Northern Hemisphere. These sources are rarely included in global dust models, even though they appear important for the climate system and contribute substantially to dust in the Arctic (Bullard et al., 2016; Groot Zwaaftink et al., 2016). Especially Icelandic deserts are known to be highly active and a high-resolution surface type map for Iceland can therefore be included in FLEXDUST simulations (Arnalds et al., 2016; Groot Zwaaftink et al., 2017). Like in FLEXPART, nested meteorological fields

25 can be used for specific regions of interest. The size distribution of emitted dust follows Kok (2011), is independent of friction velocity and is by default represented by ten size bins. This can be changed depending on known properties or assumptions of dust sources. The dust particles are assumed to be spherical in FLEXPART. An example of annual mean dust emission from 1990 to 2012 calculated with FLEXDUST driven with ERA Interim meteorology is shown in Fig. 6. Further details on FLEXDUST, including model evaluation, are given by Groot Zwaaftink et al. (2016). The source code is available from the git

30 repository: https://git.nilu.no/christine/flexdust.git.
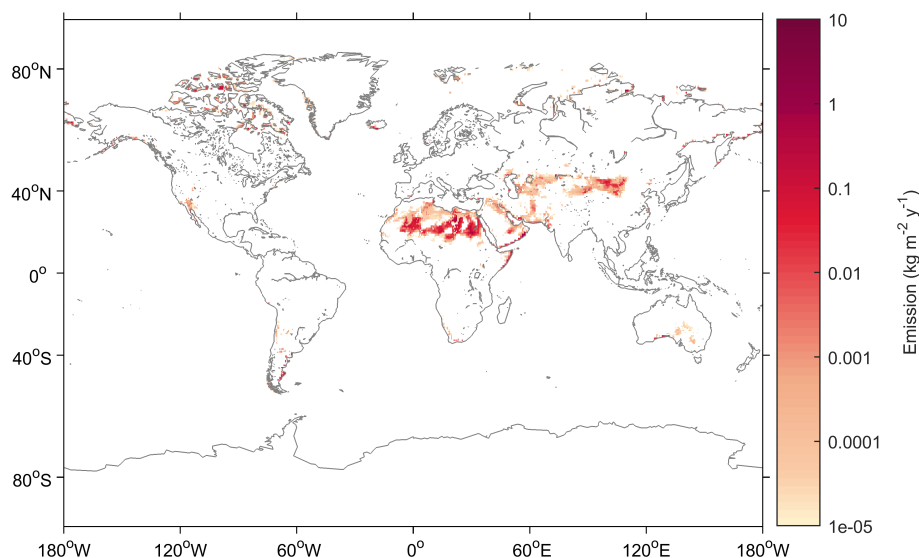
Figure 6. Average annual dust emission for the period 1990-2012 estimated with FLEXDUST driven with ERA-Interim meteorology.

3 Parallelization

In a Lagrangian model like FLEXPART, particles move totally independent of each other. This facilitates efficient paralleliza-tion of the code. The most simple and often most effective way is running several instances of the model in parallel. For example, if the model is to be run backwards (say, for 10 days) at regular intervals from a measurement site for a year, one
5 could run the model separately, in parallel, for monthly sub-periods. The total computation time of the twelve monthly pro-cesses together is nearly the same as if the model is run as one process for the whole year. Some overhead in processing input data occurs because, in the above example, 10 extra days of data per process are needed to calculate trajectories 10 days back into the preceding month. One disadvantage of that approach is that the memory needed for holding the meteorological input data and the model output fields is multiplied. However, this overhead is often small; thus, this approach has been used very
10 often by FLEXPART users in the past.

Even if a task cannot easily be decomposed into runs for different periods or sources, trivial parallelization is still possible if a large number of particles is desired, for example in a domain-filling simulation, where tens of millions of particles may be used. The strategy in this case would be to assign a fraction of the particles to each run. Note that different random seeds should be used for each run, which requires a manual change and recompilation of the code.

15 As a user-friendly alternative, FLEXPART v10.3 has been parallelized using standard parallelization libraries. Common parallelization libraries are Open Multi-Processing (OpenMP; http://www.openmp.org/) designed for multi-core processors with shared memory and Message Passing Interface (MPI, 2015) for distributed memory environments. Examples of other

Lagrangian particle models that have been parallelized are NAME (Jones et al. , 2007), which utilizes a pure OpenMP approach, and FLEXPART-WRF (Brioude et al., 2013), which uses a hybrid approach (OpenMP + MPI). For FLEXPART v10.3 we decided to use a pure MPI approach, for the following reasons:

– It is simpler to program than a hybrid model, and more flexible than a pure OPENMP model.

5   – While OPENMP in principle may be more effective in a shared memory environment, MPI can often perform equally well or better provided there is not excessive communication between the processes.

– MPI offers good scalability and potentially low overhead when running with many processes.

3.1 Implementation

The FLEXPART code contains several computational loops over all the particles in the simulation, which is where most

10 of the computational time is spent for simulations with many particles. The basic concept behind our parallel code closely resembles the "trivial parallelization" concept described above. When launched with a number of processes, N_p, each process will separately calculate how many particles to release per location, attempting to achieve an approximately even distribution of particles among the processes while keeping the total number of particles the same as for a simulation with the serial version. Each running process will generate an independent series of random numbers and separately calculate trajectories and output

15 data for its set of particles. Explicit communications between processes are only used when the output fields are combined at the master process (MPI rank 0) using `MPI_Reduce` operations, before writing the output. Also, in the case where output of all individual particle properties is desired (option `IPOUT1 = 1` or `2` in file `COMMAND`), we let each process append its data to the same file. We thus avoid the costly operation of transferring particle properties between processes. The performance of the implementation is discussed in section 3.2 (see Fig. 7).

20   Some parts of the code are not simply loops over particles, most notably the routines for reading and transforming the input meteorological data. It follows that the performance gain of using parallel FLEXPART in general is better for simulations with larger number of particles. We have, however, implemented a feature where instead of having each MPI process read and process the same input data, one dedicated MPI process is set aside for this purpose. When the simulation time t lies in the interval between wind field time T_i and T_{i+1}, all other processes calculate particle trajectories while this dedicated process

25 ingests input fields from time T_{i+2}. At simulation time $t = T_{i+1}$ the dedicated "reader process" will distribute the newest data to the other processes and immediately start reading fields for time T_{i+3}, while the other processes continue doing trajectory calculations. A hardcoded integer (`read_grp_min` in file `mpi_mod.f90`) is used to set the minimum number of total MPI processes for which this separate process will be reserved for reading input data. For the examples shown in section 3.2 a value of 4 was used (Fig. 7 and 8).

30 ### 3.2 Performance aspects

To assess the performance of the parallel code we performed two scaling experiments on different computational platforms.

Table 3. Computational speedup S for up to 16 processes for the two different MPI modes.

Number of processes	1	2	4	8	16
All processes read	1.00	1.89	3.30	5.76	9.16
Dedicated read process	1.00	1.91	3.09	6.72	13.10

3.2.1 Single node, multiple cores

In the following we present the results from running the code on a machine equipped with an Opteron 6174 processor with 16 cores. Compilation was done using `gfortran` version 4.9.1 and Open MPI version 1.8.3. For the experiment, 40 million particles were released and propagated 48 hours forwards in time. We ran with this setup with increasing number of processes, from 1 to 16. All time measurements in the code were made with the `MPI_wtime()` subroutine.

For the first experiment, every process separately processed the meteorological input data. Figure 7 (left column) shows the CPU time T_n used in the case of n processes, and the relative speedup factor $S(n) = T_1/T_n$. Time and speedup shown for "particle loops" includes the three most computationally demanding particle loops (integration of the Langevin equation, wet deposition, and concentration calculations), but in addition, FLEXPART contains a few smaller loops over particles that exhibit similar performance improvements. We see that for 40 million particles, the loops over particles take the largest share, at least 87 % of the total time when run with one process. Close-to-perfect speedup is expected and observed for these loops (compare results for "Particle loops" and "Ideal (particle loops)" in Fig. 7, left panels). The major bottleneck for overall performance in this case is that each process reads the same input files from disk, thus forcing the others to wait. This bottleneck causes the speed-up to deviate substantially from the ideal situation when more than a few processes are used (compare results for "Total" and "Ideal" in Fig. 7, left panels).

Next we repeat the experiment above but set aside a dedicated process for reading the meteorological data whenever $n \geq 4$. The results are shown in Figure 7 (right column). Numerical values for the speedup factors for selected numbers of processes are given in Table 3. We observed that with $n \geq 7$ there was consistently a benefit to setting aside the dedicated reader process, whereas for $n < 7$ it was more effective to have all processes read data and thus an extra process available for doing the trajectory calculations. These results will of course vary with the resolution of the input data, the number of particles, and the system on which the program is run.
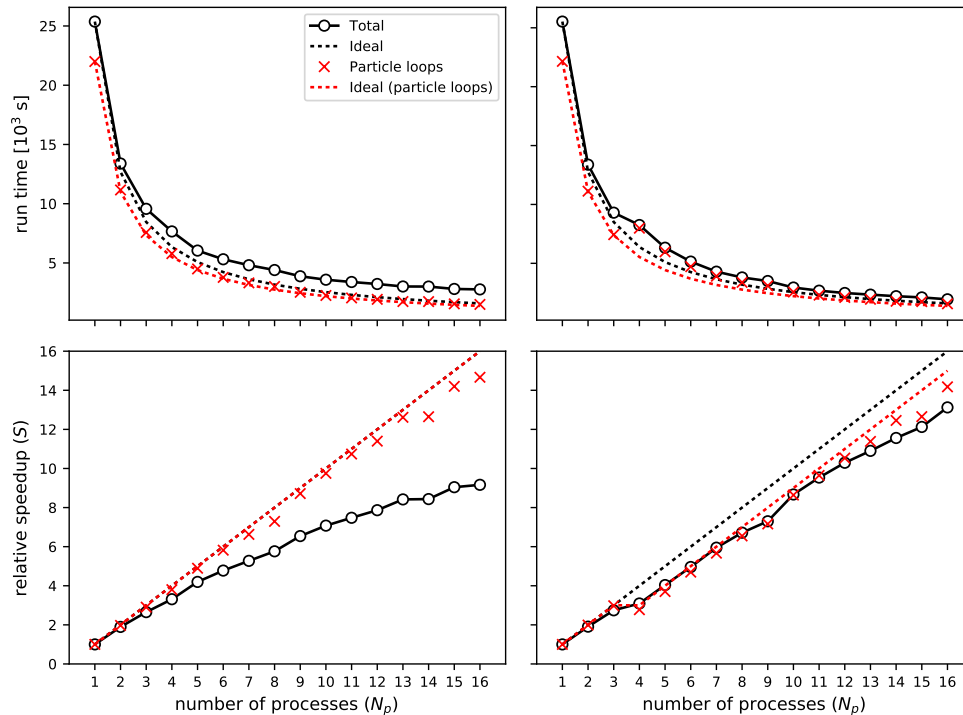
Figure 7. Computational time (top) and speedup (bottom) for up to 16 processes on a single node. On the left side, all processes read meteorological input data, whereas on the right, a dedicated process reads and distributes input data for $N_p \geq 4$

3.2.2 Multiple nodes, multiple cores

We performed a larger-scale experiment at the Abel computer cluster[1], using up to 256 cores on Intel Xeon E5-2670 CPUs. The FLEXPART setup was similar to the previous single-node experiment, but we increased the number of particles to 500 million and reduced the simulated time to 12 h. Compilation was done with Intel Fortran v16.0.1 and Open MPI v1.10.2.

5   Run time and speedup factors are shown in Table 4 and Figure 8. As before we see essentially perfect speedup of the computationally intensive parts (the particle loops), which is expected. Table 4 also gives the parallel efficiency, which is seen decreasing for larger N_p. This is partly due to the increased cost of MPI communications, and also because the non-parallel parts of the code have relatively higher impact. With 256 processes there are only about 2 million particles per process and the CPU time is not as clearly dominated by the particle loops as when 500 million particles all run in one process. In addition, the

10   initialization of the code (allocation of arrays, reading configuration files) takes around 20 s for this run, which is significant given a total runtime of 299 seconds. Thus, parallel efficiency would increase for longer simulation times and/or for simulations with more particles per process, i.e. realistic cases that are more likely to be run with such a large number of processes.

---

[1]Owned by the University of Oslo and Uninett/Sigma2, and operated by the Department for Research Computing at USIT, the University of Oslo IT-department. http://www.hpc.uio.no/

Table 4. Run time and speedup for the multi-node experiment.

Number of processes n	1	2	4	8	16	32	64	128	256
Total run time in s	39536	19681	14123	6380	3061	1568	828	491	299
Speedup factor S	1.00	2.01	3.37	6.20	12.92	25.22	47.76	80.53	132.12
Parallel efficiency (S/n)	1.000	1.004	0.843	0.775	0.807	0.788	0.746	0.629	0.516
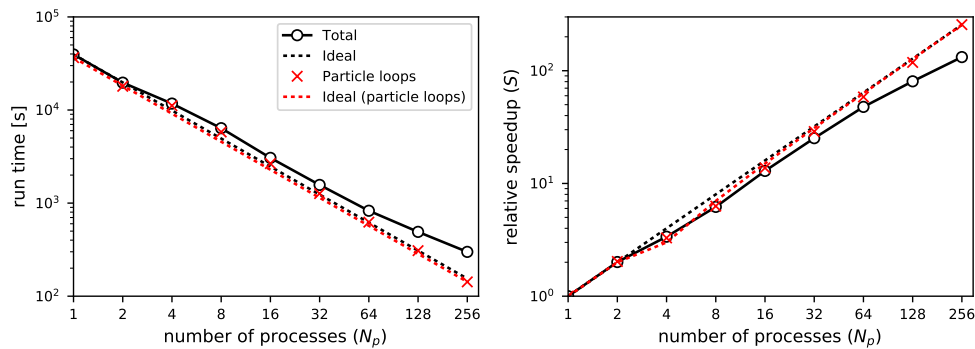
Figure 8. Computational time (left) and speedup (right) for up to 256 processes on 16 nodes. Logarithmic scaling along both axes. For $n \geq 4$ a dedicated process reads and distributes input data.

3.3 Validation

In order to ensure that the parallel version produces results with an accuracy comparable to the serial version, we have per-formed a set of tests and validation experiments. A direct comparison between the versions is difficult because FLEXPART utilizes Gaussian distributed random numbers for calculating turbulent velocities of the particles. For the parallel version we let

5 each process independently calculate a set of random numbers, which leads to small numeric differences between the versions.

To confirm that the only source of differences between the serial and parallel code is in the random number generation, we first observe that when the parallel executable is run using only one process, it produces results identical to the serial version. This is as expected, as the first MPI process (rank 0) always uses the same random number seeds as the serial version.

Next, we have done tests where all random numbers are set to 0 in both codes, corresponding to switching off the turbulent

10 displacements, and we run the parallel version using multiple processes. The outputs from the serial and parallel versions of the code when run this way are identical except for small differences due to round-off errors (e.g. in concentration calculations – these round-off errors are typically larger in the serial version due to the larger number of particles).

4   Installation, compilation and execution

FLEXPART is usually used in a Linux environment, which we also assume for the following instructions. However, the model has been implemented successfully also under MacOS and MS-Windows. The default Fortran compiler for FLEXPART v10.3 is gfortran, but ifort, Absoft and PGI compilers have been used as well.

4.1   Required libraries and FLEXPART download

As the meteorological data from numerical weather prediction models is usually distributed in GRIB format, a library for reading GRIB data is required. It is recommended to use `ecCodes`[2], the primary GRIB encoding/decoding package used at ECMWF (recent enough versions of its predecessor `grib_api`, no longer supported after 2018, can also be used). Data in GRIB-2 format can be compressed. If this is the case for the input data, the `jasper` library is needed[3]. If it is desired to produce FLEXPART output in the NetCDF format, the NetCDF Fortran Library[4] is also required.

In order to obtain the FLEXPART source code, download the appropriate v10.3 tarball from the FLEXPART website[5] and unpack it:

```
tar -xvf flexpart10.3.tar
```

or clone the FLEXPART git repository to obtain the latest available model version from the FLEXPART community website.

```
git clone https://www.flexpart.eu/gitmob/flexpart
```

After unpacking the tarball or cloning the repository, a local directory structure as shown in Table 1 is created. The directory `src` contains the code and a makefile. The makefile needs to be adapted to the compiler and libraries present on the local system. Annex A4 describes these steps in detail, including manual installation of the libraries. This was tested for Ubuntu 16.04.3 LTS Linux and MacOS (Darwin Kernel Version 14.5.0). Both a serial and a parallel executable can be built from the FLEXPART v10.3 source files.

4.2   Compiling and running the serial version

After correctly setting the library paths in the makefile, the command `make` produces the executable called `FLEXPART`. It can be executed from the command line by `./FLEXPART` and then expects a file `pathnames` to exist in the current working directory. This file contains the information, where input data are located and where output data shall be produced (see section 5). Note that `pathnames` is expected in the directory from which FLEXPART is started, which can be different from where the executable file is located. A different name of a `pathnames` file can be also given as an argument. FLEXPART thus can be invoked according to the generic syntax

```
path_to_flexpart/flexpart_executable path_to_pathnames/pathnames_file
```

---

[2]https://software.ecmwf.int/wiki/display/ECC

[3]`jasper` is available as a package in Linux distributions. https://github.com/mdadams/jasper

[4]https://www.unidata.ucar.edu/software/netcdf/

[5]https://flexpart.eu/. The website provides additional information that can be used to supplement these intructions.

Using a second argument, $-v$ (verbose mode), will display additional information during the run. Even more information including clock time between different programme units will be printed with $-v2$. Invoking FLEXPART with the flags $-i$ and $-i2$ (info mode) will provide detailed run specific information while reading input files. However, in this mode FLEXPART then stops before particle trajectories are calculated.

4.3 Compiling and running the parallel version

Most subroutines calling MPI functions are in a single module named `mpi_mod.f90`. Other FLEXPART source files that depend on this module are given a `_mpi.f90` suffix to distinguish them from the serial version. During compilation the makefile selects the source files automatically depending on whether the parallel or serial version is built.

In order to compile and run the parallel version, a MPI library must be installed, either as a package from the distribution or built from source code. Both OpenMPI[6] and mpich2[7] work but testing on some systems indicates slightly better performance with OpenMPI. As for the other libraries, the MPI library names and paths need to be adapted in the makefile. The `MPIF90` variable sets the Fortran compiler wrapper (usually `mpifort` or `mpif90`; in the case of co-existing OpenMPI and mpich installations, wrappers called `mpif90.openmpi` or `mpif90.mpich` may be defined). Compilation of the parallel version should then be done by

```
make mpi
```

This will produce an executable file `FLEXPART_MPI`. If executed, this will run on a single processor and should produce results identical to the serial version. To activate the parallel features, the executable must be run through a MPI launcher (here it is important to use the launcher corresponding to the MPI library that was used for the compilation), for example

```
mpirun -n <number> FLEXPART_MPI
```

where `<number>` specifies the number of processes one wishes to launch. For some installations, `mpirun` is called `mpiexec`, or, in the case of co-existing OpenMPI and mpich2 installations, `mpiexec.openmpi` or `mpiexec.mpich2`, respectively. Many command-line options exist for `mpirun` that can be helpful for improving performance, e.g. processor-binding. For a list of these options see `mpirun --help`.

5 FLEXPART input

In this section, we describe the different FLEXPART input files and, where appropriate, changes that have occurred since the last publication (Stohl et al., 2005). FLEXPART needs the following three types of input files:

1. The text file `pathnames` is located by default in the directory where FLEXPART is executed. It must contain at least four lines: first, the path to the directories where run-defining input files are located (the so-called `options` directory); second, the path where output files are created; third, the path to the meteorological input GRIB files; and, fourth, the

---

[6]http://www.open-mpi.org/software/ompi/v1.8/

[7]http://www.mpich.org/downloads/

Table 5. Alphabetical list of the run-defining input files (upper part) and static input files (lower parts), usually contained in a directory called `options`. Processing of files marked with † depends on the run specifications. The other files are always read in.

File name	Content
AGECLASSES†	Age-class definitions
COMMAND	Main control parameters
OUTGRID	Output grid definition
OUTGRID_NEST†	Nested output grid definition
RECEPTORS†	Receptor locations for receptor kernel output
RELEASES	Specification of the sources (forward run) or receptors (backward run)
SPECIES/	Directory containing files with definitions of physical and chemical parameters of species referenced in RELEASES
IGBP_int1.dat	Land cover input data
surfdata.t	Roughness length, leaf area index for different land cover types
surfdepo.t	Seasonal surface resistances for different land cover types
OH_variables.bin†	OH field

    path to the so-called `AVAILABLE` file (see point 3). The last two lines can be repeated if nested input data shall be used. For each nesting level, one line for the GRIB data directory and one for the corresponding `AVAILABLE` file are needed.

2. The files containing the run-defining settings are located in a subdirectory (given in line 1 of `pathnames`) by default called `options` (see Table 1). The settings, which control FLEXPART's physics and programme flow, are stored in different text files listed in Table 5 and described in section 5.1. In addition, the `options` directory contains data files that are not usually changed by the user.

3. The meteorological input data, one file for each input time, are stored in GRIB format in a common directory (specified in line 3 of `pathnames`). To enable FLEXPART to find these files, a file usually named `AVAILABLE` (given in line 4 of `pathnames`) contains a list of all available meteorological input files and their corresponding time stamps. Additional files containing nested input data may also be provided. In this case, a separate file containing the input file names (e.g. named `AVAILABLE_NESTED`) must be given. Date and time entries in the `AVAILABLE*` files for mother and nested fields must be identical. Details on the meteorological input data are given in section 5.2.

5.1 Run-defining settings: the `options` directory

Here, we give an overview of the information provided in the run-defining FLEXPART user input files listed in Table 5. In previous versions of FLEXPART, these files were formatted text files (coming alternatively in a long and a short format). For backward compatibility, these plain text formats are still supported. However, FLEXPART v10.3 also allows to use namelists,

a standard Fortran feature where values are provided in a list with elements of the form `name=value`. When FLEXPART is started, it tries to open the files as namelists, and if this is not working, it expects the files to be in one of the two old plain text formats. We encourage users to update their input files to namelists, for two reasons. Firstly, FLEXPART now has default user options for all input settings, so that users only need to set those options that they want to deviate from the defaults. Secondly,

5   namelists make it easier to add new user options, which may be required in future versions of FLEXPART. Thus, plain text input files may not be supported in future versions of FLEXPART. Examples for all formats of the user input files are contained in the FLEXPART distribution.

To convert user input files of any format to namelist format, the switch `nmlout=.TRUE.` (in file `com_mod.f90`) must be set before compilation. Then, run-defining user input files are written out in namelist format in the `output` directory, with the

10   appendix `.namelist` added to the input file name (e.g. `COMMAND.namelist`). This feature also improves the traceability of FLEXPART model results and makes simulations easily reproducible by documenting the settings used for the model run.

In the following, we provide reference tables of the run-defining user input files including default settings (in square brackets) when using the namelist format. Notice that the default values are appropriate for regional-scale simulations but simulations on smaller scales or with higher accuracy may need adjustments (in particular, shorter time steps and use of the new CBL

15   scheme).

5.1.1   File `COMMAND`

The `COMMAND` file contains the user settings controlling the simulation and the behaviour of the run. The default `COMMAND` file contains a namelist `&COMMAND`, for which Table 6 provides a complete listing of all settings, their meaning and pre-set default values. It is important that users of previous FLEXPART versions who choose to use plain text input files update their

20   `COMMAND` file, since new parameters have been added. However, the `cblflag` (and any option added afterwards) must be provided in namelist format in any case.

5.1.2   File `RELEASES`

The `RELEASES` file contains the information related to when and where the particles are introduced in the simulation and other properties of the release points (e.g. the chemical species simulated). It consists of a namelist `&RELEASES_CTRL` which

25   specifies header information. The header gives the total number of different species (i.e. different substances) to be released, followed by a corresponding list of the FLEXPART species numbers nnn, where `SPECIES_nnn` files define the species' physical properties (see section 5.1.3). Following the header, there is an arbitrary number of namelists `&RELEASE` defining each release. For each such release, the following is given: the starting and ending time, the location and extension, the masses released (one value for each released species), and the number of particles to be released, as well as a comment string. The

30   content of the `RELEASES` file is summarised in Table 7.

	Variable Name	Description	Value [default]
1	LDIRECT	Simulation direction in time	1 (forward) or -1 (backward)
2	IBDATE	Start date of the simulation	YYYYMMDD: YYYY=year, MM=month, DD=day
3	IBTIME	Start time of the simulation	HHMISS: HH hours, MI=minutes, SS=seconds. UTC zone.
4	IEDATE	End date of the simulation	Same format as IBDATE
5	IETIME	End time of the simulation	Same format as IBTIME
6	LOUTSTEP	Interval of model output	Average concentrations are calculated
			every LOUTSTEP [10800 seconds] .
7	LOUTAVER	Concentration averaging interval, instantaneous for value of zero	[10800 seconds]
8	LOUTSAMPLE	Numerical sampling rate of output, higher statistical accuracy with shorter intervals	[900 seconds]
9	ITSPLIT	Time constant for particle splitting (particles are split in two after given time)	[999999999 seconds]
10	LSYNCTIME	All processes are synchronized to this time interval,	[900 seconds]
		it has to divide all values above	
11	CTL	Factor by which particle transport time step in the ABL must be smaller than	>1 for time steps shorter than t_l.
		the Lagrangian time scale t_l; resulting time steps can be shorter than	If CTL<0, a purely random walk
		LSYNCTIME; LSYNCTIME is used if CTL<0.	simulation is done [-5.0]
12	IFINE	Additional reduction factor for time step used for vertical transport	Positive integer [4]
		only considered if CTL>1.	
13	IOUT	Switch determining the output type	[1] mass concentration (residence time backwards),
			2 volume mixing ratio, 3 both 1 and 2, 4 plume trajectories,
			5 both 1 and 4. Add 8 for NetCDF output
14	IPOUT	Switch for particle position output	[0] no particle output,
			1 particle output every output interval,
			2 only at the end of the simulation (useful, e.g. for warm start)
15	LSUBGRID	Increase of ABL heights due to sub-grid scale orographic variations	[0]=off, 1=on
16	LCONVECTION	Switch for convection parameterization	0=off, [1]=on
17	LAGESPECTRA	Switch for calculation of age spectra (needs file AGECLASSES)	[0]=off, 1=on
18	IPIN	Warm start simulation, re-started from a particle dump	[0]=no, 1=yes
		(needs partposit_end file from previous simulation)	
19	IOER	Separate output fields for each location in the RELEASE file	[0]=no, 1=yes
20	IFLUX	Output of mass fluxes through output grid box boundaries	[0]=off, 1=on
		(northward, southward, eastward, westward, upward and downward)	
21	MDOMAINFILL	switch for domain-filling calculations: particles are initialised	[0]=no, 1 like air density, 2 stratospheric ozone tracer
		to reproduce air density or stratospheric ozone density;	
		for limited-area simulations, particles are generated at the domain boundaries	
22	IND_SOURCE	Unit to be used at the source, see Seibert and Frank (2004); Eckhardt et al. (2017)	[1]=mass, 2=mass mixing ratio
23	IND_RECEPTOR	Unit to be used at the receptor, see Seibert and Frank (2004); Eckhardt et al. (2017)	[1]=mass, 2=mass mixing ratio
24	MQUASILAG	Quasi-Lagrangian mode to track individual numbered particles	[0]=off, 1=on
25	NESTED_OUTPUT	Switch to produce output also for a nested domain	[0]=no, 1=yes
26	LINIT_COND	switch to produce output sensitivity to initial conditions given	[0]=no, 1=mass concentration, 2=mass mixing ratio
		in concentration or mixing ratio units (in backwards mode only)	
27	SURF_ONLY	Output of SRR for fluxes only for the lowest model layer,	[0]=no, 1=yes
		most useful for backward runs when LINIT_COND set to 1 or 2	
28	CBLFLAG	Skewed rather than Gaussian turbulence in the convective ABL;	[0]=no, 1=yes
		when turned on, very short time steps should be used (see CTL and IFINE)	
29	OHFIELDS_PATH	Default path for OH file	

Table 6. Contents of the user input file COMMAND. Variable names with their meaning and all possible values are listed. Where appropriate, default values are given in brackets. Note that not all input parameter combinations are allowed.

Variable name	Description	Format, valid values, variable type
	Header (written only once and valid for all releases)	
NSPEC	total number of species	integer number
SPECNUM_REL	species numbers in dir `SPECIES`	integer array of size NSPEC
	For each release	
IDATE1	Release start date	YYYYMMDD: YYYY=year, MM=month, DD=day
ITIME1	Release start time in UTC	HHMISS: HH hours, MI=minutes, SS=seconds; integer
IDATE2	Release end date	Same format as IDATE1
ITIME2	Release end time in UTC	Same format as ITIME1
LON1	Left longitude of release box	-180 < LON1 <180; real
LON2	Right longitude of release box	Same format as LON1; real
LAT1	Lower latitude of release box	-90 < LAT1 < 90; real
LAT2	Upper latitude of release box	Same format as LAT1; real
ZKIND	Reference level	1=above ground, 2=above sea level, 3 for pressure in hPa; integer
Z1	Lower height of release box	Meters above reference level; real
Z2	Upper height of release box	Meters above reference level; real
PARTS	Total number of particles to be released	Integer $\geq$ 1
	For each species (NSPEC times)	
MASS	Total mass emitted	Real > 0
COMMENT	Comment	40-character string (e.g. name of release point)

Table 7. Contents of the user input file `RELEASES`.

5.1.3 `SPECIES` files

The subdirectory `options/SPECIES/` needs to contain one or more files named `SPECIES_nnn`. For each species nnn listed in the header section of the `RELEASES` file, such a `SPECIES_nnn` file must exist. The parameters in the `SPECIES_nnn` file, contained in the namelist `&SPECIES_PARAMS`, set the species name and define the physico-chemical properties of the species and are described in Table 8. These are important for simulating radioactive or chemical decay, wet deposition (scavenging) for gases and aerosols, dry deposition for gases and aerosols, particle settling, and chemical reaction with the OH radical. Some parameters are only necessary for gas tracers and some are only necessary for aerosol tracers, thus a namelist does not need to contain all parameters for both gases and particles. Optionally, since FLEXPART version 6.0, information about temporal emission variations can be added at the end of the file.

Notice that the format of the `SPECIES_nnn` files has changed from previous FLEXPART versions and users need to update their files accordingly. The use of `SPECIES_nnn` files from older FLEXPART versions may lead to run-time errors or erroneous results.

	Variable Name	Description	Default [unit] (type)
1	pspecies	Tracer name	[no units] (string)
2	pdecay	Species half life for radioactive or chemical decay; off if `pdecay<0`	[seconds] (real)
3	pweta_gas	Gases wet deposition: Below-cloud scavenging parameter A (for precip. of 1mm/h)	[1/s] (real)
4	pwetb_gas	Gases wet deposition: Below cloud scavenging parameter B (dependency on precip. rate)	[none] (real)
5	pcrain_aero	Aerosols wet deposition: Below-cloud scavenging rain collection efficiency moderator for rain C_{rain}	[none] (real)
6	pcsnow_aero	Aerosols wet deposition: Below-cloud scavenging rain collection efficiency moderator for snow C_{snow}	[none] (real)
7	pccn_aero	Aerosols wet deposition: In-cloud scavenging, cloud condensation nuclei efficiency CCN_{eff}	[none] (real)
8	pin_aero	Aerosols wet deposition: In-cloud scavenging, ice nuclei efficiency IN_{eff}	[none] (real)
9	preldiff	Gases dry deposition: Ratio $D = D_{H_2O}/D_i$, D_{H_2O} of the diffusivity of H_2O to the diffusivity of the component D_i	[none] (real)
		Dry deposition of gases is switched off by negative D.	
10	phenry	Gases dry deposition and in-cloud scavenging: Henry's constant H	[M/atm] (real)
11	pf0	Gases dry deposition: Reactivity factor for oxidation of biological substances relative to that of ozone.	$0 \leq f_0 \leq 1$ [none] (real)
		For non-reactive species f_0 is 0, for slightly reactive species it is 0.1 and for highly reactive species it is 1.	
12	pdensity	Aerosols dry deposition and settling: Particle density ρ	[kgm^{-3}] (real)
13	pdquer	Aerosol dry deposition, aerosol wet deposition: below cloud scavenging: Particle mean diameter $\bar{d}$. Decides whether its gas(<=0) or aerosol (>0)	[m] (real)
14	psigma	Aerosol dry deposition: Species diameter standard deviation	[m] (real)
15	pdryvel	Gases dry deposition: Dry deposition velocity (only used if `preldiff` and `pdensity` < 0)	[m/s] (real)
16	pweightmolar	Gases: Species molar weight. Used for volume mixing ratio (pptv) output	[g/mol] (real)
17	pohcconst	Gases OH reaction: C	[cm^3/molecule/s] (real)
18	pohdconst	Gases OH reaction: D	[K] (real)
19	pohnconst	Gases OH reaction: N	[none] (real)
20	parea_hour	Emission variation factor (area source) for hour of the day, starting with 0-1 local time, 24 values	[1] (real)
21	parea_dow	Emission variation factor (area source) for day of the week, starting with Monday, 7 values	[1] (real)
22	ppoint_hour	Emission variation factor (point source) for hour of the day, starting with 0-1 local time, 24 values	[1] (real)
23	ppoint_dow	Emission variation factor (point source) for day of the week, starting with Monday, 7 values	[1] (real)

Table 8. FLEXPART variables set in the user input file `SPECIES_nnn` for species number nnn. Note that the variable names given in the input namelist are the same as used subsequently in FLEXPART but with a prepended letter p (for parameter). For instance, `pspecies` corresponds to `species`.

The following specifies the parameters associated to each physico-chemical process simulated:

5   – Radioactive or chemical decay: set with `pdecay`, off if `pdecay<0`.

    – Wet deposition for gases: set with `pweta_gas`, `pwetb_gas` (for below-cloud) and `phenry` (for in-cloud), off if either `pweta_gas` or `pwetb_gas` is negative.

    – Wet deposition for aerosols set with: `pccn_aero`, `pin_aero` for in-cloud scavenging, and `pcrain_aero`, `pcsnow_aero`, `pdquer` for below-cloud scavenging.

10   – Dry deposition for aerosols set with: `pdensity`, `pdquer` and `psigma`, off if `pdensity`< 0.

- Dry deposition for gases set with: `phenry`, `pf0` and `preldiff`; off if `preldiff`<0. Alternativley, a constant dry deposition velocity `dryvel` can be given.

- Settling of particles set with: `pdensity` and `dquer`.

- OH reaction: Chemical reaction with the OH radical can be turned on by giving parameter `pohcconst` (cm^3 molecule^{-1} s^{-1}), `pohdconst` (K) and `pohnconst` (no unit) positive values, defined by Eq. 13.

- Emission variation: Emission variation during the hours (local time) of the day and during the days of the week can be specified. Factors should be 1.0 on average, to obtain unbiased emissions overall. The area source factors (useful, e.g. for traffic emissions) are applied to emissions with a lower release height below 0.5 m above ground level (agl) and the point source factors (useful, e.g. for power plant emissions) to emissions with a lower release height above 0.5 m agl. Default values are 1.0.

5.1.4 File `OUTGRID`

The `OUTGRID` file specifies the domain and grid spacing of the three-dimensional output grid. Note that in a Lagrangian model, the domain and resolution of the gridded output is totally independent from that of meteorological input (apart from the fact that the output domain must be contained within the computational domain). The `OUTGRID` file contains a namelist `&OUTGRID` specifying all parameters. The variables read in for this file and all the following input files have not changed in recent FLEXPART versions; thus, for more explanations, see Stohl et al. (1995). Example files can be found in the `options` directory in the `FLEXPART` distribution.

5.1.5 File `OUTGRID_NEST`

Output can also be produced on one nested output grid with higher horizontal resolution, defined in the file `OUTGRID_NEST`, but with the same vertical resolution as given in `OUTGRID`. The `OUTGRID_NEST` file contains a namelist `&OUTGRIDN` specifying all parameters.

5.1.6 File `AGECLASSES`

The option to produce age class output can be activated in the `COMMAND` file. The file `AGECLASSES` then allows to define a list of times (in seconds, in increasing order) that define the age classes used for model output. With this option, the model output (e.g. concentrations) is split into contributions from particles of different age, defined as the time passed since the particles' release. Particles are dropped from the simulation once they exceed the maximum age, allowing their storage locations to be re-used for new particles. This is an important technique to limit the memory usage for long-term simulations. Thus, even if the user is not interested in age information per se, it may often be useful to set one age class to define a maximum particle age.

5.1.7 File **RECEPTORS**

In addition to gridded model output, it is also possible to define receptor points. With this option output can be produced specifically for certain points at the surface in addition to gridded output. The RECEPTORS file contains a list with the definitions of the receptor name, longitude and latitude. If no such file is present, no receptors are written to output.

5.1.8 Static data input files

Several files contain static input data that are not usually modified by the user. These are (by default) also located in the options directory. If modelling of a species requires calculating OH reactions, an OH field stored in file OH_variables.bin needs to be present. The file IGBP_int1.dat is a land cover inventory, file surfdata.t gives the roughness length and leaf area index of the different land cover types, and file surfdepo.t contains surface resistances for dry deposition calculations.

5.2 Meteorological data and pre-processing routines

FLEXPART can be run with meteorological input data for global domains or for smaller, limited area domains. The FLEXPART computational domain always corresponds to this mother domain set by the input data, while the output domain can be smaller. FLEXPART can also ingest higher-resolution meteorological input data in sub-domains of the mother domain. Such nested data must be available for the exact same times as those for the mother domain, checked by FLEXPART by comparing the time stamps in the two AVAILABLE(_NESTED) files. There is no nesting in the vertical direction and the poles must not be contained in any nest. To automatically produce the AVAILABLE(_NESTED) files, a python script is available from the FLEXPART website[8] which checks which input files are present and then creates this file in the required format.

Compilation of FLEXPART v10.3 produces a single executable that automatically detects whether the meteorological input data comes from ECMWF-IFS or NCEP-GFS, and whether they are in GRIB-1 or in GRIB-2 format. Nevertheless, certain parameters may need to be adapted in par_mod.f90 to the size of the meteorological input files (array dimensions) and the input grid may need to be shifted relative to the output grid (parameter nxshift). In the following, we describe how meteorological input data appropriate for FLEXPART can be retrieved from ECMWF and NCEP.

5.2.1 ECMWF data retrieval

ECMWF data can be comprised of analysis and/or forecast data from the operational IFS data stream or specific reanalysis projects. For operational data, the meteorological fields can currently have a temporal resolution of up to 1 hour, a vertical resolution of 137 model levels and $0.1° \times 0.1°$ horizontal resolution on a regular latitude-longitude grid. Other ECMWF data sets can have coarser resolution. For example, ERA-Interim re-analysis data (Dee et al., 2011) with up to $0.75° \times 0.75°$ latitude/longitude resolution and 60 vertical levels can be retrieved 3-hourly by mixing 6-hourly analysis and 3-hour forecast fields. The new Copernicus reanalysis ERA5 provides 1-hourly analysis fields with 137 model levels and a horizontal resolu-

---

[8]https://flexpart.eu/wiki/FpInputMetMkavail, last access: 25 June 2018

tion of 31 km ($0.28125°$). Notice that access to some data sets, in particular the operational forecasts, is restricted and requires specific access[9]. However, reanalysis data[10] are available publicly.

The IFS is a global model that uses spectral representation with spherical harmonics for the dynamical part and a grid-point representation on a reduced Gaussian grid for the physical part. However, FLEXPART needs the input data on a regular latitude-
5 longitude grid and thus IFS data have to be pre-processed. With respect to the vertical coordinate system, the data needs to be on the native ECMWF model levels (η levels) which are subsequently transformed within FLEXPART to a terrain-following vertical coordinate system.

As explained above, each ECMWF dataset has its own specific temporal and spatial resolution and the meteorological parameters provided can be different from dataset to dataset. To produce meteorological GRIB files suitable for FLEXPART input
10 from these different datasets, a software called `flex_extract` (current version 7.0.4) has been developed specifically for this purpose. In order to prepare the GRIB files from ECMWF's Meteorological Archival and Retrieval System (MARS[11]), several retrieval requests using the MARS command language and some further processing steps are needed. Since all ECMWF data sets need to be handled differently and some may not even contain all information needed for FLEXPART, `flex_extract` has a focus on some of the most important ones for driving FLEXPART. These are, in particular, the reanalysis datasets ERA-
15 Interim (Dee et al., 2011), CERA-20C (the coupled climate reanalysis of the 20th century; Laloyaux et al. , 2018) and also the latest reanalysis ERA5 as well as data from the operational IFS stream. Each file (one for each time step) prepared by `flex_extract` for FLEXPART consists of a set of model level and surface data as a combination of analysis and forecast fields depending on availability. For example, certain variables such as precipitation may only be available in forecast fields, whereas other data are also contained in analysis fields. `flex_extract` seeks an optimum combination of such data. Note
20 that some parameters are stored as time-accumulated fields in the ECMWF archives and `flex_extract` calculates the instantaneous fluxes out of them (e.g. precipitation fluxes). For more details on this process of de-accumulation see Hittmeir et al. (2018). Since FLEXPART needs the pressure hybrid coordinate vertical velocity as used in the ECMWF model, an important feature of `flex_extract` is the computation of this parameter from the horizontal wind field (see Stohl et al., 2001) for ERA-Interim and for the years when it was not operationally archived in MARS (before 2009).

25 ECMWF is a European intergovernmental organisation which grants full access to its multi-petabyte MARS archive for their member and co-operating states. Users with a full-access account can run `flex_extract` v7.0.4 directly on ECMWF servers or via a local gateway server. This mode is required for retrieving also the most recent operational data from ECMWF. Users from member or co-operating states interested in this mode should contact the computing representative from their national meteorological service to obtain an account. Users from other countries worldwide can self-register at ECMWF for a public
30 account to be able to retrieve the public datasets (i.e. most reanalysis products). `flex_extract` v7.0.4 makes use of the WebAPI[12] tool provided by ECMWF to access the data from outside their systems. This tool can distinguish between public and member state users. Therefore, it is also a convenient option for member and co-operating state users who only need data

---

[9]https://www.ecmwf.int/en/forecasts/accessing-forecasts, last access: 23 June 2018

[10]https://software.ecmwf.int/wiki/display/WEBAPI/Available+ECMWF+Public+Datasets, last access: 23 June 2018

[11]https://software.ecmwf.int/wiki/download/attachments/45759146/mars.pdf, last access: 24 June 2018

[12]https://software.ecmwf.int/wiki/display/WEBAPI/ECMWF+Web+API+Home, last access: 24 June 2018

older than a few days from the operational stream or reanalysis data. A full-access account to ECMWF servers is no longer needed in this case.

`flex_extract` v7.0.4 is a set of Python routines combined with a Fortran programme for faster computation of grid transformations and vertical velocity calculation. A Python 2.7 interpreter with several common modules, such as NumPy and

5   datetime, are required and usually included in the Anaconda distribution[13]. Additionally, a Fortran compiler, the ECMWF Web API tool, the GRIB-API or ecCodes module and the Emoslib interpolation library have to be available. Note that the GRIB-API (or ecCodes) module has to be available for Python as well as for Fortran. Installation instructions can be found at ECMWF websites directly or in the Software Installation Plan for `flex_extract`. Knowledge of Python, although helpful, is not necessary for using the retrieval scripts. A certain knowledge of the ECMWF dataset to be retrieved is useful to understand

10 the composition of retrievals but many basic examples of CONTROL files are provided in the `flex_extract` distribution. These CONTROL files determine the key parameters for the `flex_extract` MARS retrievals and can be adapted to change domain, and spatial and temporal resolution. Even for these few parameters the user should check for availability upfront. For example, ERA-Interim data has a maximum grid resolution of 0.75° x 0.75° and 6-hourly temporal resolution for the public dataset. The usage scenarios of the `flex_extract` v7.0.4 retrieval scripts are summarised in Fig. 9.

15 The `flex_extract` v7.0.4 software is included in the FLEXPART v10.3 file tree under the directory `preprocess` (see Table 1). It can also be downloaded from https://flexpart.eu/[14] as a tar-ball and used as a standalone package. For more details the reader is referred to the `flex_extract` v7.0.4 user documentation (e.g. Software Installation Plan (SIP.pdf) and the Software User Tutorial (SUT.pdf)) in `preprocess/flex_extract`.

5.2.2   NCEP data retrieval

20 Meteorological data from NCEP's GFS are freely available and easily accessible and are ingested by FLEXPART on pressure levels, unlike ECMWF data. These pressure level data have lower resolution than model level data but offer the advantage of great consistency between different data sets. Therefore, pre-processing of NCEP data is much more simple than that of ECMWF data, and limited to precipitation data, which are available only in forecast fields.

Both operational analysis data and several re-analyses data sets are available. Notice that NCEP also provides forecast data

25 for free, which are not available from ECMWF even for member-state users except for national meteorological services or users with a special contract. The data retrieval from NCEP is described in a wiki page on the FLEXPART web site[15], where also a script for downloading NCEP data can be found. Operational GFS data can be downloaded by simple ftp or wget from a rolling archive of the meteorological forecast and analysis data[16]. Six-hourly NCEP FNL (Final) Operational Model Global Tropospheric Analyses[17] are available in near-real time since July 1999. These data are similar to the operational analyses, but

---

[13]https://www.anaconda.com/download/, last access: 25 June 2018

[14]https://flexpart.eu/downloads/61, last access: 8 July 2018

[15]https://flexpart.eu/wiki/FpInputMetGfs (last access 8 July 2018)

[16]http://www.ftp.ncep.noaa.gov/data/nccf/com/gfs/prod/ (lastaccess8July2018), under the catalogue `gfs.YYYYMMDDHH`, which contains fields in GRIB-2 format

[17]http://rda.ucar.edu/datasets/ds083.2/
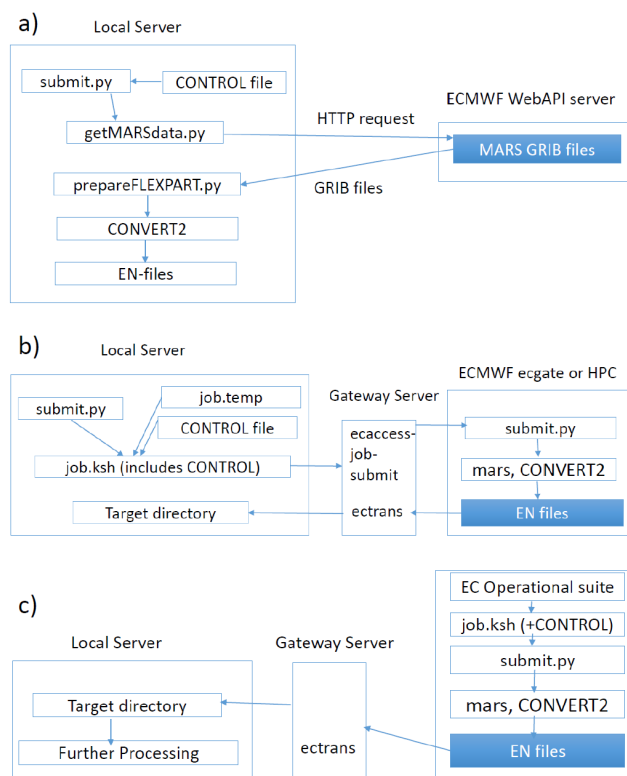
Figure 9. Summary of the flex_extract retrieval script usage scenarios. Scenario a) applies to any user worldwide. Scenario b) is for users with log in access to the ECMWF archives. Scenario c) is appropriate for operational use of (near) real time data.

NCEP ingests also late-incoming observation data for their production. Archived re-analysis datasets are also available from NCEP, e. g. the Climate Forecast System Reanalysis (CFSR) Selected Hourly Time-Series Products[18] for the period January 1979 to March 2011.

6   FLEXPART output

5 ## 6.1   Output files overview

In the following we describe the FLEXPART output files together with changes made since the last documented FLEXPART version (Stohl et al., 2005). An overview of all possible output files is provided in Table 9. Notice that not all these files are written out in every model run; the user settings control which files are produced. At the beginning of a run, FLEXPART records descriptive metadata in the binary file `header`. This information is also written into the plain-text files

---

[18]http://rda.ucar.edu/datasets/ds093.1/

`header_txt` (with the exception of the orography data and the releases information). The releases information is written in `header_txt_releases`. Corresponding files `header_nest`, etc. are produced if nested output is selected.

Table 9. List of FLEXPART output files and for which user settings ("switches") they are produced. See Table 10 for details on the units in the gridded output.

name	format	switches	description of contents
header	binary	default output	run metadata + ancillary data
header_txt	text	default output	human readable run metadata (from COMMAND)
header_txt_releases	text	default output	human readable run metadata (from RELEASES)
dates	text	default output	Time series: dates of output files
grid_conc_date_nnn	binary (sparse array)	LDIRECT=1 IOUT=1, 3, 5	3D tracer mass density + 2D deposition
grid_pptv_date_nnn	binary (sparse array)	LDIRECT=1 IOUT=2, 3	3D tracer mass density + 2D deposition
grid_time_date_nnn	binary (sparse array)	LDIRECT=-1 IOUT=1	3D sensitivity of atmospheric receptor to emissions
grid_drydep_date_nnn	binary (sparse array)	LDIRECT=-1 IOUT=1, IND_RECEPTOR=3	3D sensitivity of dry deposition receptor to emissions
grid_wetdep_date_nnn	binary (sparse array)	LDIRECT=-1 IOUT=1, IND_RECEPTOR=4	3D sensitivity of wet deposition receptor to emissions
grid_conc_date_nnn.nc	binary (NetCDF)	LDIRECT=1 IOUT=9,11,13	3D tracer + 2D wet and dry deposition
grid_time_date_nnn.nc	binary (NetCDF)	LDIRECT=-1 IOUT=9	3D sensitivity of atmospheric receptor to emissions
grid_drydep_date_nnn.nc	binary (NetCDF)	LDIRECT=-1 IOUT=9, IND_RECEPTOR=3	3D sensitivity of dry deposition receptor to emissions
grid_wetdep_date_nnn.nc	binary (NetCDF)	LDIRECT=-1 IOUT=9 , IND_RECEPTOR=3	3D sensitivity of wet deposition receptor to emissions
grid_initial_nnn	binary (sparse array)	LDIRECT=-1, LINIT_COND>0	3D sensitivity of receptor concentrations/deposition to initial conditions
partposit_date	binary	IPOUT=1,2	particle positions
		IPOUT=1,2 MQUASILAG=1	particle positions numbered consecutively
trajectories.txt	text	IOUT=4, 5	clustered trajectories
receptor_conc	binary	LDIRECT=1 IOUT=1, 3, 5, 9, 11, 13	mass density at receptors
receptor_pptv	binary	LDIRECT=1 IOUT=2, 3, 9, 11	volume mixing ratio at receptors
header_nest	binary	NESTED_OUTPUT=1	nest metadata + ancillary data
grid_conc_nest_date_nnn	binary (sparse array)		
grid_pptv_nest_date_nnn	binary (sparse array)	as for mother grid	as for mother grid in a
grid_time_nest_date_nnn	binary (sparse array)	+ NESTED_OUTPUT=1	higher resolution latitude-longitude grid
grid_drydep_nest_date_nnn	binary (sparse array)		
grid_wetdep_nest_date_nnn	binary (sparse array)		
grid_conc_nest_date_nnn.nc	binary (NetCDF)		
grid_time_nest_date_nnn.nc	binary (NetCDF)		
grid_drydep_nest_date_nnn.nc	binary (NetCDF)		
grid_wetdep_nest_date_nnn.nc	binary (NetCDF)		

At each output time, FLEXPART produces files containing the gridded output. Separate files are created for every species and domain (mother and, if requested, nest). The naming convention for these files is `grid_type_date_nnn`. For forward runs, `type` can be `conc` and `pptv` for concentrations and mixing ratios, or `flux` for 3D mass fluxes across the grid cell faces (Stohl et al., 2005, sect. 8.5). For backward runs, `type` can be `time` for sensitivity of receptor concentrations to emission fluxes, `drydep` for sensitivity of receptor dry deposition to emissions, or `wetdep` for sensitivity of receptor wet deposition to emissions. For backward runs, there can also be an output file `grid_initial_nnn`, which gives the receptor sensitivity

to initial conditions. `date` denotes the date and time for which the output is valid, and `species` is the species number as specified in `RELEASES`. The list of the output times is progressively written to the text file `dates`. For the nested output, `grid` is replaced by `grid_nest`.

Wet and dry deposition fields in forward runs are calculated on the same horizontal output grid and are appended to
5 `grid_conc_date_nnn` and `grid_pptv_date_nnn` files. The deposited matter is accumulated over the course of a model run. It generally increases with model time but for species with radioactive decay, losses are possible. As for long simulations small deposition amounts may be added to already large deposited quantities, the default precision of the deposition fields was changed from single (in older FLEXPART versions) to double precision to avoid numerical inaccuracies when deriving instantaneous fluxes from accumulated quantities.

10 For a list of points at the surface, concentrations or mixing ratios in forward simulations can also be calculated independently from the grid using a kernel method and recorded in the files `receptor_conc` and/or `receptor_pptv`.

If the particle dump option is activated, in addition to the gridded output, the particle coordinates together with additional variables such as pressure, humidity, density, tropopause height, ABL height and orography height are recorded in the binary files `partposit_date`. These data can be useful for a variety of different purposes, for instance diagnostics of the water
15 cycle (Stohl and James, 2004). If plume trajectory mode is activated, for every release the positions of trajectory clusters representing the centres of mass of all released particles are recorded in the file `trajectories.txt` (Stohl et al., 2002, 2005, sect. 10).

The physical unit used for the output data in the files `grid_conc_date_nnn` and `grid_time_date_nnn` depends on the settings of the switches `ind_source` and `ind_receptor`, following Table 10. Noteworthy, the unit used in `grid_conc_date_nnn`
20 can also be a mass mixing ratio. For forward runs, additional files `grid_pptv_date_nnn` can be created (setting `IOUT` to values of 2 or 3), which contain data as volume mixing ratios (requires molar weight in `SPECIES_nnn` file). Source-receptor relationships (i.e. emission sensitivities) in backward mode for atmospheric receptors are written out in `grid_time_date_nnn` files, those for deposited mass are recorded in files `grid_wetdep_date_nnn` and `grid_drydep_date_nnn` (see Seibert and Frank (2004); Eckhardt et al. (2017) and section 2.4, and Table 10 for output units). Notice that the user can also
25 provide different input units. For instance, if emissions in a forward run are specified in Becquerel (Bq), the output would be in nBq m^{-3} with `ind_source`=1 and `ind_receptor`=1. Notice further that all gridded output quantities in FLEXPART are grid-cell averages, not point values.

6.2 Sparse matrix output

Depending on the type of model run, the gridded output can contain many grid cells with zero values (e.g. dispersion from a
30 point source, backward run from a single receptor). The output is therefore written in a sparse-matrix format which is specific to FLEXPART. The array containing the data to be written out is scanned for sequences of non-zero values. The number of sequences found is stored in an integer variable `sp_count_i`, and the field positions where each sequence begins is stored in a 1-D integer array `sparse_dump_i`, using a one-dimensional representation of the output field. The total number of nonzero values is stored in `sp_count_r` and the nonzero values themselves in the real vector `sparse_dump_r`. Since all

Table 10. Physical units of the input (in file `RELEASES`) and output data for forward (files `grid_conc_date_nnn`) and backward (files `grid_time_date_nnn`) runs for the various settings of the unit switches `ind_source` and `ind_receptor` (for both switches, 1 refers to mass units, 2 to mass mixing ratio units). `IOUT` is 1 (or 9 for NetCDF output) except where indicated. "(dep.)" in lines 5 and 6 of the table refer to the deposition output provided in addition to the atmospheric output in files `grid_conc_date_nnn`.

Direction	file name	ind_source	ind_receptor	input unit	output unit
Forward	`grid_conc*`	1	1	kg	$ng\,m^{-3}$
	`grid_conc*`	1	2	kg	ppt by mass
	`grid_conc*`	2	1	1	$ng\,m^{-3}$
	`grid_conc*`	2	2	1	ppt by mass
	`grid_conc*`	1	1 or 2 (dep.)	kg	$ng\,m^{-2}$
	`grid_conc*`	2	1 or 2 (dep.)	1	$ng\,m^{-2}$
	`grid_pptv*` (IOUT=2, 3)	1	1	1	ppt by volume
Backward	`grid_time*`	1	1	1	s
	`grid_time*`	1	2	1	$s\,m^3\,kg^{-1}$
	`grid_time*`	2	1	1	$s\,kg\,m^{-3}$
	`grid_time*`	2	2	1	s
	`grid_wetdep*`	1	3 (wet dep.)	1	m
	`grid_drydep*`	1	4 (dry dep.)	1	m
	`grid_wetdep*`	2	3 (wet dep.)	1	$kg\,m^{-2}$
	`grid_drydep*`	2	4 (dry dep.)	1	$kg\,m^{-2}$
	`grid_initial*`	1	1	1	1
	`grid_initial*`	1	2	1	$m^3\,kg^{-1}$
	`grid_initial*`	2	1	1	$kg\,m^{-3}$
	`grid_initial*`	2	2	1	1

physical output quantities of FLEXPART are greater than or equal to zero, nonzero sequences are stored in `sparse_dump_r` with alternating signs which allows to separate different sequences upon reading. Finally, all four variables are written out to the unformatted output file. This format replaces the compression used up to version 7 (the smallest of a full dump and a simple sparse matrix format) saving up to 60% of disk space. The sparse matrix data can be read for example with the functions

5   `readgrid.f` (Fortran) and `flex_read.m` (MATLAB) described in section 6.4

6.3 NetCDF output

FLEXPART v10.3 can also support output in NetCDF format if the NetCDF libraries are available. To activate NetCDF support, append `ncf=yes` to the verb|make| command. If FLEXPART is compiled and linked to the NetCDF libraries, output files in NetCDF format can be produced by adding 8 to the `IOUT` parameter in the input file `COMMAND`, e.g. `IOUT=9` corresponds

Table 11. Additional information in the NetCDF output file as attributes.

Conventions	CF-1.6 (NetCDF CF convention identifier)
Title	FLEXPART model output (content title)
Institution	producer string 'institution' set in `netcdf_output_mod.f90`
Source	creation string 'flexversion' model output set in `FLEXPART.f90`
History	date string with login and host name
References	Stohl et al., Atmos. Chem. Phys., 2005, doi:10.5194/acp-5-2461-200

to `IOUT=1` with the standard binary output, see Tables 9 and 5.1.1. In the NetCDF module `netcdf_output_mod.f90` a parameter `write_releases` determines at compile time if the information on the releases should also be written to the NetCDF file. Only one NetCDF file is written which contains all species and all time steps. Both mother and nested output (if present) are contained in that file. Since the NetCDF output is specified in the Climate and Forecast (CF) format, any standard

5 software can be used for displaying and processing the output (e.g. panoply, ncview). NetCDF output data files are compressed.

The NetCDF output file contains information on the run settings and the simulation grid from the `COMMAND` and `OUTGRID*` files . It also contains additional information in the header on the producing center, as listed in Table 11. The content of these attributes can be adapted in the file `netcdf_output_mod.f90` before compilation.

6.4 Post-processing routines

10 For the NetCDF output of FLEXPART, standard visualization tools, for example Panoply, can be used. For the sparse-matrix binary output, several post-processing routines (MATLAB, Fortran, R, Python and IDL) have been developed in order to assist in the usage and analysis of these data. A number of post-processing tools are available on-line (https://flexpart.eu/wiki/FpOutput, last access: 16 Aug 2018). Note that some of these tools require to read a text-string containing the model version. Since the length of this string changed in FLEXPART v9.2, the post-processing routines now require the allocation of a longer

15 string.

Fortran routines are available for download on the FLEXPART website with the subroutines `readheader.f` for reading the header, and `readgrid.f` for reading the gridded binary fields. Analysis or plotting programmes written in Fortran can call these subroutines.

There are also MATLAB tools working in a similar way as the Fortran routines, with `flex_header.m` for reading the

20 header and `flex_read.m` for reading the data fields. If particle dumps were made, the MATLAB function `readpart.m` reads the corresponding data files (a similar Fortran code is also available).

The R programmes available for post-processing FLEXPART output include routines to read the binary output in the `grid_conc` (or `grid_pptv`) and `grid_time` files and to plot maps. Routines are also available to plot trajectories on a map from the file `trajectories.txt` and to plot time series of concentrations (or mixing ratios) from the file

25 `receptor_conc` (or `receptor_pptv`).

Several Python tools are available for reading FLEXPART data from release 8.0 and above. The module `reflexible`, available from the FLEXPART website and also at https://github.com/spectraphilic/reflexible (last access: 6 Aug 2018) enables the user to easily read and access the header and grid output data of the FLEXPART model runs. It provides a simple tool that facilitates consistent reading of both the original sparse matrix output files as well as the NetCDF output. Some basic plotting

5   functionality is provided to quickly assess and validate runs or to look at the input parameters. An alternative Python tool is `Quicklook` that can be also downloaded from the Flexpart website.

7   Application examples

In this section we provide 37 examples of the FLEXPART model that serve three purposes: 1) verification of a new FLEXPART installation; 2) demonstration of the model capabilities for new users; 3) confirmation of consistency in the model output when

10   code changes are made that should not change the results. These examples do not represent an exhaustive set of all possible model uses, but they are designed to demonstrate and test different widely used functionalities of the model.

All examples are variations of a default example case, which uses the settings in the user input files as distributed with the FLEXPART v10.3 code package. These default input files are located in the directory `options` (section 5) and are consistent with the default meteorological data retrieved from ECMWF by the `flex_extract` package (Appendices A5 and B1). An

15   `AVAILABLE` file fitting with these input data is also distributed with FLEXPART. These default settings are described in detail in Appendix B2.

Using the default example as a basis, the different functionalities of the model can be activated by adequately changing certain parameters in the user input files, thereby generating 36 other example runs. We have categorised these examples into ten different groups, where each group explores different capabilities of the model. Table 12 lists all examples and the parameter

20   changes needed to produce them. The first group includes the default example and explores the different options for producing gridded model output (e.g. output units, output formats) for a simple forward model run with a single starting point over the North Atlantic. The second group of examples introduces FLEXPART's backward simulation capability. The third group demonstrates different usages of the particle dump output. The fourth group gives examples for the use of mass vs. mass mixing ratio units at both the source and the receptor and for both forward and backward simulations, for establishing source-receptor

25   relationships as in Seibert and Frank (2004). The fifth group produces output for different chemical species and aerosols. The sixth group illustrates the use of nested output fields. Group seven is constituted of a single domain-filling run, as used for instance, in Stohl and James (2004). Group eight contains settings for a backward run providing 2-D sensitivities to gridded surface fluxes and 3-D sensitivities to initial conditions, as they are typically required for inverse modelling of greenhouse gases (e.g. Thompson et al., 2017). Group nine shows the use of the new skewed turbulence parameterization (Cassiani et al.,

30   2015). Group 10 contains a forward two day run simulating instantaneous emissions from a hypothetical Grimsvötn eruption (Fig. 10).

The list of examples may be extended in the future, to allow testing of even more model features, and to provide a reference archive to see how FLEXPART results may change as the code is being developed further. The user can get these reference

Table 12. List of the test cases for FLEXPART 10.3

Group	Test name	Change to default options	Description
1) gridded output	1	default (IOUT= 1)	default option: forward run with mass concentration output, see Table 10
	2	IOUT= 2	mixing ratio
	3	IOUT= 3	concentration and mixing ratio
	5	IOUT= 5	concentration and trajectory cluster
	9	IOUT= 9	mass concentration in NetCDF output format
	10	IOUT= 10	mixing ratio in NetCDF output format
	11	IOUT= 11	concentration and mixing ratio in NetCDF output format
	12	IOUT= 12	trajectory cluster
2) bwd	bwd	LDIRECT= -1	SRR
	bwd5	LDIRECT= -1, IOUT=5	backward trajectory cluster
	bwd_nc	LDIRECT= -1, IOUT= 9	SRR in NetCDF output format
3) particle	part1	IPOUT= 1	particle dump
	part2	IPOUT= 2	particle dump at end of simulation
	part_bwd1	IPOUT=1, LDIRECT= -1	backward trajectories
	part_QUASILAG	IPOUT=1, MQUASILAG=1	trajectories sequential numbering
4) units	ind_1_2	IND_RECEPTOR=2	receptor (gridded) in mass mixing ratio units
	ind_2_1	IND_SOURCE= 2	source in mass mixing ratio units
	ind_2_2	IND_SOURCE= 2, IND_RECEPTOR= 2	source and receptor in mass mixing ratio units
	bwd_ind_1_2	IND_RECEPTOR=2, LDIRECT= -1	receptor in mass mixing ratio units, backward
	bwd_ind_2_1	IND_SOURCE= 2, LDIRECT= -1	source in mass mixing ratio units, backward
	bwd_ind_2_2	IND_SOURCE= 2, IND_RECEPTOR= 2, LDIRECT= -1	source and receptor in mixing ratio units, backward
5) species	specNO	SPECNUM_REL=3	nitric oxide species
	specCO	SPECNUM_REL=22	carbon monoxide species
	specAERO-TRACE	SPECNUM_REL= 23	idealised aerosol simulation
	specBC	SPECNUM_REL=40	black carbon simulation
	bwd_specNO	SPECNUM_REL=3 , LDIRECT= -1	nitric oxide simulation backward
6) nest	nested	NESTED_OUTPUT= 1	nested output
	nested_nc	NESTED_OUTPUT=1, IOUT= 9	nested output in NetCDF format
	nested_mr	NESTED_OUTPUT= 1, IOUT= 2	volume mixing ratio nested output
	nested_mr_nc	NESTED_OUTPUT= 1, IOUT= 10	volume mixing ratio nested output netcdf
	nested_bwd	NESTED_OUTPUT= 1, LDIRECT= -1	nested output backwards
	nested_bwd_nc	NESTED_OUTPUT= 1, LDIRECT= -1 , IOUT= 9	nested output backwards in NetCDF output format
7)	DOMAINFILL	MDOMAINFILL= 1	domain filling run
8)	Gmode_bwd	LINIT_COND= 1, SURF_ONLY=1, LDIRECT= -1	sensitivity to initial conditions and surface fluxes
9) CBL	CBLFLAG	CBLFLAG=1	skewed turbulence
	CBLFLAG_bwd	CBLFLAG= 1, LDIRECT= -1	skewed turbulence backwards
10)	Volc	Modified `RELEASES` file	Hytpothetical volcanic eruption
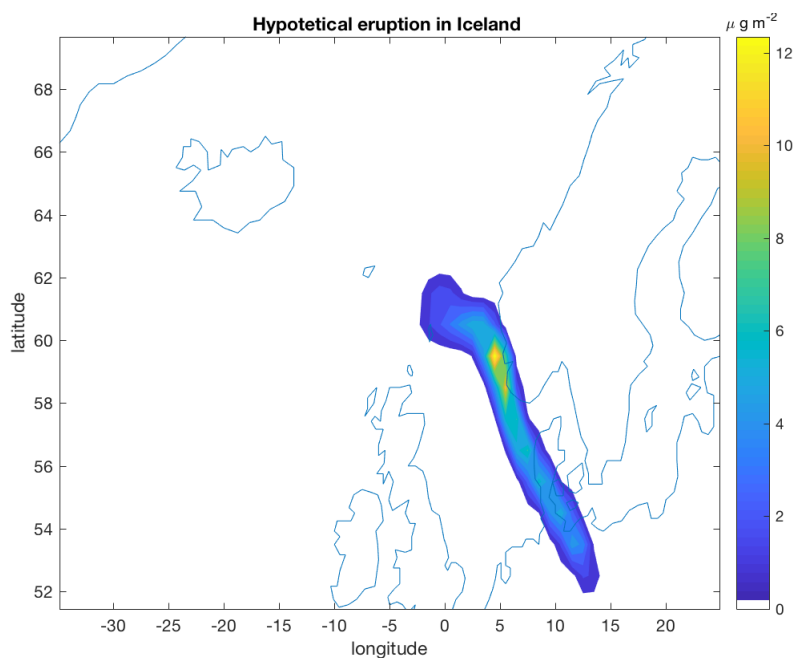
Figure 10. Hypothetical Grimsvötn eruption on 1 April 2015 at 00:00 UTC (instantaneous release). Total column concentrations are shown in μg m^{-2} 18 hours after the eruption

results and from https://flexpart.eu. A quick reference containing mean and maximum grid values for every example is also given in Appendix B5.

The directory `tests/examples/` contains scripts that generate all the files necessary to run the examples. These scripts, described in Appendix B3, generate the input files by modifying the namelists in the default `options` directory provided with

5 the distribution. This is done by the bash script `gen_options_all.sh`. For instance, the example "bwd" is generated by changing the line containing the parameter `LDIRECT` to -1 in the file `COMMAND`.

After the input data files are generated, all examples can be executed interactively from the command line. Alternatively, the script `gen_batch_jobs_cl.sh` generates a batch script for each case (to be run from the command line or using a workload manager such as SLURM). This procedure automates the sample output generation. Once the output files are created,

10 they can be read using the tools in the directory `postprocess`. They can be plotted and analysed with e.g. the reading routines described in section 6.4. In addition, some testing capabilities have been added. These are presented in Appendix B.

8 Final remarks, outlook and future code development

In this note, we have described the Lagrangian particle dispersion model FLEXPART v10.3. Two decades ago, the model code was developed mainly by one person, with specific code input from a few other researchers. At that time, no specific

15 measures were needed to ensure code consistency, track code changes, identify coding bugs, etc. However, as the number of FLEXPART users has grown substantially in recent years, more and more people have started to develop the code, contributed code snippets, and reported or identified bugs. Resulting code changes range from the adaptation of more modern coding standards, parallelization and efficiency enhancements, improvement of the model functionality, addition of output options, to revisions and extensions of the model physics. All this has been documented in this paper. Integration of all these changes into

20 a single stable model version represents a growing challenge in itself, and efforts to address this challenge (e.g. model website and repository, version control, testing environment) have also been documented here.

As FLEXPART is developed further, updates will continue to be made available on the FLEXPART website https://flexpart. eu. We encourage established and new users to contribute to FLEXPART development by providing their code changes, as well as a description of these changes, as new feature branches of the latest commits in the FLEXPART git repository. New

25 code should pass all test cases provided in the FLEXPART distribution and provide consistent output, unless there are specific reasons why output should be different, such as improvements in the model physics. This will expedite integration of important new model features in the main development branch of the model.

Code and data availability

The code and data are available from the community website http://www.flexpart.eu. The official release of FLEXPART 10.3

30 including code and data will be made available with the final version of the present work as supplementary material.

Author contributions

I. Pisso coordinated the contributions to the manuscript and the code development since version 9 including the implementation of the testing environment and the distributed version control.

E. Sollum developed and wrote the description of the parallelised version of FLEXPART and lead the assembling of the new code developments into the main model version 10.3.

H. Grythe developed and tested the new wet deposition scheme for aerosols.

N. I. Kristiansen contributed to the new wet deposition scheme for gases and performed tests of the new model version.

M. Cassiani developed the optional new turbulence scheme and the NorESM version and contributed to the WRF version.

S. Eckhardt developed and wrote the description of the backward deposition, performed the benchmark test case together with I.P. and worked on ECMWF data retrieval and testing.

D. Arnold and D Morton contributed the CTBTO developments including the unified executable the Vtables approach and testing environment.

R. L. Thompson developed the temporal variation and temperature dependence of the OH-reaction.

C. Groot Zwaaftink developed the dust mobilisation scheme around FLEXPART, and performed testing of the new model version.

N. Evangeliou tested of the new model version for black carbon and radionuclide applications.

H. Sodemann implemented the namelist input file format, and contributed to the implementation of the netCDF output and GRIB input routines.

L. Haimberger developed versions 2.0-7.02 of the `flex_extract` retrieval software, in particular the codes for calculating the hybrid coordinate vertical velocity. He also supervised the most recent developments and wrote the description together with A. Philipp.

S. Henne and D. Brunner contributed to the implementation of the netCDF output module.

J. Burkhart coordinated the development up to FLEXPART version 8.3 and contributed the post-processing Python module.

A. Foilloux developed the new Pyhton based ECMWF data retrieval software.

J. Brioude lead the developments of the WRF and ARMOME versions and contributed to the turbulence scheme.

A. Philipp developed, maintained and wrote the description of the `flex_extract` retrieval routines and contributed to the testing environment.

P. Seibert devised the community website flexpart.eu and takes care of tickets and wiki, contributed to various parts of the code development, and to editing of the manuscript.

A. Stohl developed the first version of the code in 1998 and supervised all recent developments, included the new settling parametrisation for aerosols and worked on the writing and structuring of the manuscript.

Acknowledgements. The work was performed at the Nordic Centre of Excellence eSTICC, which is supported by Nordforsk grant 57001. Funding was partly received from the European Research Council (ERC) under grant agreement no. 670462 (project COMTESSA). P. Kaufmann and M. Schraner (MeteoSwiss) are acknowledged for code re-formatting from fixed Fortran 77 to free Fortran 90 format. We thank M. Mulder for comments on an earlier version of this manuscript. The single executable and I/O improvements have been developed

5   within the project "Enhancements of the FLEXPART software on a call-off basis" (2015) funded by CTBTO. The resources for the numerical simulations were provided by UNINETT Sigma2 - the National Infrastructure for High Performance Computing and Data Storage in Norway under projects NN9419K and NS9419K. Input wind fields were provided by ECMWF.

Appendix A: Installing FLEXPART and `flex_extract`

Here, we provide step-by-step instructions on how to install FLEXPART on Linux from scratch. This has been tested on

10   an Ubuntu 16.4 distribution running on a dedicated instance in the Amazon cloud. Notice that in most environments, some or all of the required libraries (e.g. a Fortran compiler) are already installed and an installation totally from scratch would thus not be needed. In such cases, we recommend strongly that these libraries are used instead of installing everything from scratch. However, sometimes it may be necessary installing them from source (e.g. to avoid incompatibilities between different compilers or different versions of the same compiler). In the following, we assume that the user has root privileges in the system,

15   but it is also possible for normal users to install the libraries in non-standard locations. It is possible to ask for help by writing to the FLEXPART user email list (registration needed) or by creating a ticket on the community website https://flexpart.eu.

A1   Preparing the system

To begin, ensure that the latest packages are being used:

```
sudo apt-get update
```

20   The Fortran compiler is essential:

```
sudo apt-get install g++ gfortran
```

Some libraries (e.g. `grib_api`, `jasper-1.900.1`) require the GNU autotools suite in order to configure, build and install:

```
sudo apt-get install autoconf libtool automake flex bison
```

Newer packages migrate this task to cmake (e.g.):

```
sudo apt-get install cmake
```

Python is not required for FLEXPART itself but is necessary for some pre- and post-processing tools, in particular `flex_extract` for retrieving ECMWF wind fields. Git is recommended to access the code repositories. An editor (here, vim) is usually also necessary. All these packages need to be installed:

```
sudo apt-get install python-dev python-pip  git-core vim
```

A2 Installing GRIB libraries

If JPG compression is needed to decode the input meteorological winds, download the jasper library from the jasper project page[19] and install it:

```
curl https://www.ece.uvic.ca/~frodo/jasper/software/jasper-1.900.1.zip --output jasper-1.900.1.zip
5  sudo apt install unzip
   unzip jasper-1.900.1.zip
   cd jasper-1.900.1
   ./configure
   make
10 make check
   sudo make install
```

Ensure that the path `/usr/local/lib/` is in the environmental variable `$PATH`, otherwise ecCodes may not find it. Obtain and unpack ecCodes:

```
   curl https://software.ecmwf.int/wiki/download/attachments/45757960/eccodes-2.7.3-Source.tar.gz \
15 --output eccodes-2.7.3-Source.tar.gz
   tar -xvf eccodes-2.7.3-Source.tar.gz
```

Download the grib_api library from the ECMWF website[20] and install it:

```
   gunzip grib_api-X.X.X.tar.gz
   tar xf grib_api-X.X.X.tar
20 ./configure [--prefix=grib_api_dir] [--with_jasper=<jasper installation path>]
   make
   make check
   make install
```

If you have no root privileges in your system, give the full path of `grib_api_dir` to the prefix option. If jasper is in a
25 non standard location, is has to be passed to the `grib_api` configuration script. Please note that GRIB-API support will be discontinued at the end of 2018. Starting from version 2.0.0, ecCodes is the primary GRIB encoding/decoding package used at ECMWF. Any new features for the handling of GRIB files will be only developed in ecCodes.

A3 Installing NetCDF libraries

In order to enable NetCDF output, the NetCDF library has to be available in the system. For building the NetCDF library it
30 is recommended to first build HDF5 with support for compression (zlib). For this, download zlib (version 1.2.8) from the zlib website[21] and install it:

---

[19]http://www.ece.uvic.ca/ mdadams/jasper/

[20]https://software.ecmwf.int/wiki/display/GRIB/Home

[21]https://www.zlib.net/

```
tar xzvf zlib-1.2.8.tar.gz
cd zlib-1.2.8/
./configure [--prefix=<installation path>]
make
```
5 ```
make install
```

Download HDF5 from the Hdfgroup website[22] and install it:

```
tar xzvf hdf5-1.8.17.tar.gz
cd hdf5-1.8.17/
./configure --with-zlib=<path to zlib> [--prefix=<installation path>]
```
10 ```
make
make check
make install
```

Download the latest stable version of NetCDF-C from the Unidata website[23] and install it:

```
tar xzvf netcdf-4.4.1.tar.gz
```
15 ```
cd netcdf-4.4.1/
./configure --enable-netcdf-4 [--prefix=<installation path>]
make
make check
make install
```

20 Download the latest stable version of NetCDF-Fortran from the unidata website[24] and install it:

```
tar xzvf netcdf-fortran-4.4.4.tar.gz
cd netcdf-fortran-4.4.4/
./configure [--prefix=<installation path>]
make
```
25 ```
make check
make install
```

A4   Installing FLEXPART

Download the latest release of the FLEXPART source code archive from the FLEXPART homepage[25]:

```
tar -xvf flexpartXX.tar.gz
```

30 Alternatively, clone the FLEXPART repository directly from the FLEXPART community site GIT.

---

[22]https://www.hdfgroup.org/HDF5/release/obtainsrc.html
[23]https://www.unidata.ucar.edu/downloads/netcdf/
[24]https://www.unidata.ucar.edu/downloads/netcdf/
[25]https://flexpart.eu/wiki/FpDownloads

```
git clone https://www.flexpart.eu/gitmob/flexpart
```

You may need to change `makefile` in `$flexhome/src`. Edit the LIBRARY path variable in the `makefile` according to the position of `libeccodes` (or `libgrib_api`) and `libjasper`. Optionally, edit the file `par_mod.f90` to set parameters for the meteorological data, grid dimension, and maximum particle number (`maxpart`, `maxspec`, `nxmax`,

5 `nymax`, `nuvzmax`, `nwzmax`, `nzmax`, `nxshift`). The default values are set to work with the test cases of section 7 but may be too small for large simulations or too large for the available system resources. Then type:

```
make
```

in order to create the executable. Invoking the executable `FLEXPART` should now print in the standard output:

```
Welcome to FLEXPART Version 10.3
```
10 ```
FLEXPART is free software released under the GNU General Public License.
```

However, without access to valid input data, the programme will issue an error. Appendix C explains how to generate valid output with the standard meteorological fields from ECMWF that can be obtained following the procedure described in A5. The makefile also allows the command:

```
make clean
```

15 which can be used to safely remove all object and module files, e. g. if one wants to recompile after compiler option changes.

A5 Installing `flex_extract`

A short description of installation steps for this software are demonstrated for the public user mode (mode a in Fig. 9). For this mode, the user does not need to be a member state user[26] but can simply register at the ECMWF website. For the other operating modes and a more detailed explanation see the `README.md` file of the `python` directory in the `flex_extract`

20 distribution or the documentation files `SIP.pdf` and `SUT_ondemand.pdf`.

First of all, the user should register at the ECMWF website[27]. To access public datasets each dataset license has to be accepted separately before the account can be used for retrieval of these data. This can be done at the following website: https://software.ecmwf.int/wiki/display/WEBAPI/Available+ECMWF+Public+Datasets (last access: 13.10.2018).

A5.1 System preparation for `flex_extract`

25 `flex_extract` requires a Python environment and a Fortran compiler. See section A1 for installation instructions. To prepare the environment for the `flex_extract` installation, it is advisable to consider the official documentation and information from the ECMWF websites. We recommend the following steps:

1. For important information read the `Emoslib`[28] installation instructions first.

---

[26]https://www.ecmwf.int/en/about/who-we-are/member-states; last access: 13.10.2018

[27]https://www.ecmwf.int/en/forecasts/accessing-forecasts/order-historical-datasets; last access: 13.10.2018

[28]https://software.ecmwf.int/wiki/display/EMOS/Emoslib; last access 13.10.2018

2. Read the ECMWF blog about gfortran[29] for details in the installation process of the libraries.

3. Install `FFTW`[30] for Fortran, which is a library for computing the discrete Fourier transformation. This library is necessary for `Emoslib`. (Note: Apply `make` twice! Once without any options and once with single precision option, see information on `Emoslib` website).

4. Install the interpolation library `Emoslib` for Fortran.

5. Install `ecCodes`[31] or `grib_api`[32] (for python and Fortran). The `grib_api` support will be discontinued at the end of 2018 but `ecCodes` is downward compatible with `grib_api`.

6. Install the ECMWF `WebAPI`[33] client by following the instructions at the website. It is a python library to provide external access to the ECMWF servers.

7. Check whether `LD_LIBRARY_PATH` and `PATH` environment variables contain all paths to the libraries installed before! The user should modify the `.bashrc` or `.tcshrc` file to guarantee that the variables contain the paths every time a new console is used.

8. Install the python package `numpy` via pip[34].

9. Check availability of python packages (e.g. check in python console the commands: `import eccodes` / `import grib_api` / `import ecmwfapi`)

10. Start a simple test retrieval (following the instructions at the ECMWF `WebAPI` website).

11. Install `flex_extract` (see next section).

It is important to use the same compiler and compiler version for all libraries and the Fortran programme `CONVERT2`.

A5.2 Building `flex_extract`

To install `flex_extract` a script `install.py` was prepared. The user can find it in the `python` directory of the `flex_extract` distribution.

The public user mode requires a local installation of `flex_extract`. Hence, we recommend to adapt the paths to `ecCodes`, `Emoslib` or `grib_api` in one of the prepared makefiles, such as `Makefile.local.gfortran`, which can be found in the `src` directory. If a different compiler is used, this must also be adapted in the makefile. Then the installation script can be called as follows:

---

[29]https://software.ecmwf.int/wiki/display/SUP/2015/05/11/Building+ECMWF+software+with+gfortran; last access: 13.10.2018

[30]http://www.fftw.org; last access 13.10.2018

[31]https://software.ecmwf.int/wiki/display/ECC; last access 13.10.2018

[32]https://software.ecmwf.int/wiki/display/GRIB/Home; last access 13.10.2018

[33]https://confluence.ecmwf.int//display/WEBAPI/Access+MARS; last access 13.10.2018

[34]https://scipy.org/install.html; last access 13.10.2018

```
./install.py --target=local --makefile=Makefile.local.gfortran
```

With this setting `flex_extract` is installed within the current `flex_extract` directory. To install it in a different place, e. g. within a `FLEXPART` distribution, the user can set the path with the parameter `flexpart_root_scripts`. The installation was successful if the compilation of the Fortran programme (`CONVERT2`) did not fail and is displayed at the end in the
5   terminal.

A5.3   Running `flex_extract`

`flex_extract` is controlled by providing `CONTROL`-files which contain a list of parameter settings. These parameters are described in detail in the *Software User Tutorial* (`SUT.pdf`) in the `docs` directory. The `CONTROL` files specify which ECMWF dataset is to be retrieved, the time and spatial resolution, the format of the grib file, and other options. In the python di-
10 rectory are some example `CONTROL` files for the different datasets and access modes. They can be used as templates. `CONTROL` files with a `.public` ending are usable for the public access mode. The main difference is the parameter `dataset` which explicitly specifies the public data sets. Note that not all meteorological fields, times and parameters were archived in the public datasets. This is already considered in the public `CONTROL` files.

To run `flex_extract`, the main programme `submit.py` must be called. It retrieves the ECMWF data and generates
15 the FLEXPART input files. To show all possible parameter options one can use the `-h` option. The script must be called from the `python` directory of the `flex_extract` distribution. From the `-h` output it is clear that most parameters have default values or were already set via a `CONTROL` file parameter, except for the date. To retrieve just one day, one only needs to provide the start date. The rest will be done by `flex_extract`. This leads to the following script call for an arbitrary date:

```
./submit.py --controlfile=CONTROL_EI.public \
20          --start_date=20120101 \
            --public=1
```

The programme now displays each MARS request and some messages for the preparation of the `FLEXPART` input files. Eventually, the programme will finish with a `Done!` message if there was no error. Output will be stored in the default directory `work`, which is a sub-directory of the distribution directory (`flex_extract_v7.0.4`). The produced files can
25 serve as input to FLEXPART.

Appendix B: Running and testing FLEXPART

After a working FLEXPART executable is built (Appendix A), the next step is running the model and generating valid output. This requires consistent meteorological input data and user input files. In this section we describe: how to obtain the necessary wind fields (1), how to test run the executable with a default example (2), how to generate other examples (3), and how to run
30 these examples and compare them with a reference output (4). In the following, `$flexhome` indicates the path to the root

FLEXPART directory (e.g. `$HOME/flexpart/`) and `$flex_extracthome` indicates the path to the `flex_extract`
root directory (e.g. `$flexhome/preprocess/flex_extract/`).

B1   Meteorological input for the examples

Appendix A describes how to build the the `flex_extract` version included in the source code. Here, we describe the
5   settings to produce the meteorological input data required for running the default (section B2) and derived (section B3) cases.
The instructions are for ECMWF ERA5 reanalysis, which is a publicly available dataset[35]. Therefore, the data can be obtained
via ecmwfapi and no special access rights to ECMWF are needed. However, in order to retrieve the data the user needs to
register, obtain a personal ssh key and properly configure the file `.ecmwfapirc`. The execution of the retrieval requires
the Python packages `ecmwfapi` (for access) and `grib_api` (for processing). To retrieve the data, execute the following
10   commands:

```
export PYTHONPATH=path/to/ecmwfapi:path/to/grib_api
$flex_extracthome/Python>./submit.py --start_date 20170102  --controlfile CONTROL_EA5
```

This should generate the files `EA170102??` in the directory

`$flex_extracthome/work/`

An `AVAILABLE` consistent with these wind fields is shipped together with the FLEXPART distribution:

`$flexhome/AVAILABLE`

B2   Running the default example: installation verification

With the input files, which are included in the FLEXPART distribution and described in section 5, a first test case to see if
15   FLEXPART was installed correctly can be run. For starting the model run, the meteorological data has to be in `$flex_extracthome/wo`
(see B1), the file `pathnames` in `$flexhome`, and the executable in `$flexhome/src/`. In the `$flexhome` directory type:

`$flexhome>./src/FLEXPART`

The results created by this run are stored in the directory `$flexhome/output` (as defined in `pathnames`). The run should
end with the following message:

```
CONGRATULATIONS: YOU HAVE SUCCESSFULLY COMPLETED A FLEXPART MODEL RUN!
```

If this message is received, the model has completed the simulation, which confirms that FLEXPART and all required libraries
20   are installed correctly. However, it does not guarantee valid output. To verify that the results obtained are valid, see section B5.

B3   Generating variations of the default example

To demonstrate more functionalities, a set of shell scripts generating different FLEXPART setups are provided in `$flexhome/tests/ex`
The script `set_default_example.sh` takes the content of the `options` directory and `pathnames` file from B2 as a ba-
sis and then `gen_options_all.sh` creates new `options_suffix` directories for all of the cases described in Table 12.

---

[35]https://confluence.ecmwf.int/display/WEBAPI/Access+ECMWF+Public+Datasets

Here, suffix corresponds to the example name as given in column 2 in Table 12. Finally, the script `gen_pathnames.sh` generates corresponding `pathnames_suffix` files pointing to all the `options_suffix` directories. With this, all example cases of Table 12 are ready to run.

B4 Running the examples

5 The examples can be run interactively one by one by invoking FLEXPART with the corresponding `pathnames_suffix` file. Alternatively, the script `gen_batch_jobs_cl.sh` generates a one line script for each example case containing a call of FLEXPART and the appropriate `pathnames_suffix` file as a command line parameter. All example scripts can then be run sequentially with `run_batch_cl.sh`, which creates `output_suffix` directories with the results, as well as log files `batch_job_pathnames_suffix.stdout` for each run. The examples described above can now be read and plotted 10 with the tools included in the distribution. All of the files and directories created by executing the scripts from B2 to B4 can be removed again with the command `make clean`.

B5 Comparing the results

To verify that FLEXPART is producing valid output, it is useful to compare the output of a new installation with existing model output. It is also useful to repeat such a comparison after code changes, to make sure the output is not affected, except for model 15 simulations where changes in the results are intended. While comprehensive comparisons of model results are possible, here we provide only a very simple way of checking the model results. The file `gridded_output.txt` contained in the FLEXPART distribution contains, for all the examples that produce gridded output, the mean and the maximum value that occurs in the gridded output files. This shall serve as a reference to which users can compare their results to and thus verify that the model produces output as expected.

Appendix C: FLEXPART model versions

20 In addition to the reference version of FLEXPART described in this paper, there exist many different model branches that were developed either for special purposes or to ingest other meteorological input data. This appendix provides an incomplete list and a short description of some of these other versions. Further contributions are welcome in order to keep this list up to date.

C1 FLEXPART-NorESM/CAM

25 Recently, a FLEXPART model version FLEXPART-NorESM/CAM was developed, which is tailored to run with the meteorological output data generated by the CMIP5-version of NorESM1-M (the Norwegian Earth System Model) with $1.89° \times 2.5°$ horizontal resolution and 26 vertical levels. FLEXPART-NorESM/CAM is based on FLEXPART V9, and the atmospheric component of NorESM1-M is based on CAM4 (the Community Atmosphere Model). The adaptation of FLEXPART to NorESM required new routines to read meteorological fields, new post-processing routines to obtain the vertical velocity in

the FLEXPART coordinate system and other changes, detailed by Cassiani et al. (2016). The code can be downloaded from https://www.flexpart.eu/wiki/FpClimateNorESM.

C2 FLEXPART-WRF

This FLEXPART version uses output from the Weather Research and Forecasting (WRF) mesoscale meteorological model
5 (Brioude et al., 2013). Originally it was developed at PNNL (Pacific Northwest National Laboratory) and named PILT (PNNL Integrated Lagrangian Transport). Compared to PILT, the further developed FLEXPART-WRF can use both instantaneous and time-averaged meteorological output of the WRF model. The latest version also includes the skewed turbulence scheme that was subsequently ported to the standard FLEXPART version 10.3. FLEXPART-WRF output can either be in binary or Network Common Data Form (NetCDF) format, both of which have efficient data compression. FLEXPART-WRF also offers effective
10 parallelisation with Open-MP in shared memory and MPI library in distributed memory. Released versions of the code can be downloaded from https://www.flexpart.eu/wiki/ or cloned from the open repositoy git@git.nilu.no:flexpart/flexpart-wrf.git.

C3 FLEXPART-COSMO

In Europe several national weather services and research groups develop and operate the non-hydrostatic limited-area atmospheric model COSMO (Consortium for Small-scale Modeling). At MeteoSwiss COSMO is operationally run with data
15 assimilation on two grids with approximately 7×7 km^2 and 2×2 km^2 horizontal resolution centered over Switzerland. This enables the study of atmospheric transport over complex terrain on a long-term basis. To this end, we have developed a new version of FLEXPART that is offline coupled to COSMO output (FLEXPART-COSMO hereafter) and supports output from multiple COSMO nests. Particles are internally referenced against the native vertical coordinate system used in COSMO and not, as in standard FLEXPART, in a terrain following z-system. This eliminates the need for an additional interpolation step.
20 A new flux de-accumulation scheme was introduced that removes the need for additional preprocessing of the input files. In addition to the existing Emmanuel based convection parameterisation, a convection parameterisation based on the Tiedtke scheme, which is identical to the one implemented in COSMO itself, was introduced. A possibility for offline nesting of a FLEXPART-COSMO run into a FLEXPART-ECMWF run for backward simulations was developed that only requires minor modifications of the FLEXPART-ECMWF version and allows particles to leave the limited COSMO domain. The OpenMP
25 shared-memory parallelisation to the model allows for asynchronous reading of input data. The code is available on request from dominik.brunner@empa.ch and stephan.henne@empa.ch.

C4 FLEXPART-AROME

The Applications of Research to Operations at Mesoscale (AROME) numerical weather prediction model is run operationally by Météo France at mesoscale. AROME forecasts for Europe exist at a resolution of 1.3×1.3 km^2. Based on FLEXPART-WRF,
30 a coupling between FLEXPART and AROME is under development at Laboratoire de l'Atmosphère et des Cyclones (LACy, a joint institute between CNRS, Météo-France and University of Reunion island) using AROME high-resolution (2.5×2.5 km^2)

forecasts over the Southwest Indian Ocean. This branch simulates turbulent transport using the Thomson turbulent scheme (Thomson, 1987). already implemented by Lin et al. (2003) in the stochastic time-inverted Lagrangian transport (STILT) model. This method constrains mass transport between different turbulent regions to conserve mass locally for a passive well-mixed tracer. Turbulent kinetic energy profiles are taken directly from AROME model outputs. Such treatment of turbulent

5   motion ensures consistency between the turbulence in the meteorological fields calculated by the NWP model and turbulence computed in the offline Lagrangian transport model. It has been noticed that the the use of a dedicated ABL scheme such as Hanna in the FLEXPART model may generate inconsistency between the ABL turbulent domain and the resolved wind fields used to drive FLEXPART. Simulations using the Thompson scheme show better representation of the turbulent mixing between boundary layer air and free tropospheric air.

10   **C5   TRACZILLA**

This fork from FLEXPART version 5 was originally developed for studies of transport and mixing in the upper troposphere-lower stratosphere region (e.g. Legras et al. (2003); Pisso and Legras (2008)). The modifications from FLEXPART advection scheme consists mainly in discarding the intermediate terrain following coordinate system and in performing a direct vertical interpolation of winds, linear in log-pressure, from hybrid levels. The vertical velocities are computed by the FLEXPART

15   preprocessor using a mass conserving scheme in the hybrid ECMWF coordinates. Alternatively the vertical velocities can be computed from the rates of diabatic heating from ECMWF winds. In addition to the reanalyses from ECMWF, the current version can use MERRA (Modern-Era Retrospective analysis for Research and Applications) from NASA and JRA-55 (the Japanese 55-year Reanalysis) from JMA. The parallelisation uses the OMP version of PGI. All arrays are allocated dynamically. The code can be obtained from https://github.com/bernard-legras/traczilla.

References

Asman, W. A. H.: parametrisation of below-cloud scavenging of highly soluble gases under convective Atmos. Environ., 29, 1359–1368, 1995.

Arnalds, O., P. Dagsson-Waldhauserova, and H. Olafsson: The Icelandic volcanic aeolian environment: Processes and impacts—A review, Aeolian Res., 20, 176–195, doi:10.1016/j.aeolia.2016.01.004, 2016.

Arnold, D., C. Maurer, G. Wotawa, R. Draxler, K. Saito, P. Seibert: Influence of the meteorological input on the atmospheric transport modelling with FLEXPART of radionuclides from the Fukushima Daiichi nuclear accident, Journal of Environmental Radioactivity, 139, 212–225, https://doi.org/10.1016/j.jenvrad.2014.02.013, 2015.

Atkinson, R. : Gas-phase tropospheric chemistry of volatile organic compounds: 1. Alkanes and alkenes, Journal of Physical and Chemical Reference Data, 26(2), 215-290, 1997.

Bey I, Jacob DJ, Yantosca RM, et al.: Asian chemical outflow to the Pacific in spring: Origins, pathways, and budgets. J. Geophys. Res., 106, 19, 23073-23095, 2001.

Brioude, J., Arnold, D., Stohl, A., Cassiani, M., Morton, D., Seibert, P., Angevine, W., Evan, S., Dingwell, A., Fast, D. J., Easter, R. C., Pisso, I., Burkhart, J. and Wotawa, G.: The Lagrangian particle dispersion model FLEXPART-WRF version 3.1. Geosci. Model Dev. 6, 1889-1904, doi:10.5194/gmd-6-1889-2013, 2013.

Bullard, J. E., Baddock, M., Bradwell, T., Crusius, J., Darlington, E., D. Gaiero, Gasso, S., Gisladottir, G., Hodgkins, R., Mc- Culloch, R., Neuman, C. M., Mockford, T., Stewart, H., and Thorsteinsson, T.: High latitude dust in the earth system, Rev. Geophys., 54, 447–485, https://doi.org/10.1002/2016RG000518, 2016.

Cassiani, M, Stohl, A. and Brioude, J.: Lagrangian stochastic modelling of dispersion in the convective boundary layer with skewed turbulence conditions and a vertical density gradient: Formulation and implementation in the FLEXPART Model. Boundary-Layer Meteorology, 154, 367–390, doi:10.1007/s10546-014-9976-5, 2015.

Cassiani, M., Stohl, A., Olivié, D., Seland, Ø., Bethke, I., Pisso, I., and Iversen, T.: The off-line Lagrangian particle model FLEXPART-NorESM/CAM (V1): model description and comparisons with the on-line NorESM transport scheme and with the reference FLEXPART model, Geosci. Model Dev. Discuss., doi:10.5194/gmd-2016-86, in review, 2016.

Cozic, J., Verheggen, B., Mertes, S., Connolly, P., Bower, K., Petzold, A., Baltensperger, U. and Weingartner, E.: Scavenging of black carbon in mixed phase clouds at the high alpine site Jungfraujoch, Atmospheric Chemistry and Physics, 7(7), 17971807, doi:10.5194/acp-7-1797-2007, 2007.

Dee, D. P., Uppala, S. M., Simmons, A. J., Berrisford, P., Poli, P., Kobayashi, S., Andrae, U., Balmaseda, M. A., Balsamo, G., Bauer, P., Bechtold, P., Beljaars, A. C. M., van de Berg, L., Bidlot, J., Bormann, N., Delsol, C., Dragani, R., Fuentes, M., Geer, A. J., Haimberger, L., Healy, S. B., Hersbach, H., Hólm, E. V., Isaksen, L., Kallberg, P., Köhler, M., Matricardi, M., McNally, A. P., Monge-Sanz, B. M., Morcrette, J.-J., Park, B.-K., Peubey, C., de Rosnay, P., and Tavolato, C., Thépaut, J.-N., and Vitart, F.: The ERA-Interim reanalysis: configuration and performance of the data assimilation system. Q. J. R. Meteorol. Soc., 137, 553-597, 2011. doi: 10.1002/qj.828

Eckhardt, S., Prata, A. J., Seibert, P., Stebel, K., and Stohl, A.: stimation of the vertical profile of sulfur dioxide injection into the atmosphere by a volcanic eruption using satellite column measurements and inverse transport modeling. Atmos. Chem. Phys., 8, 3881–3897, 2008.

Eckhardt, S., Cassiani M., Evangeliou N., Sollum E., Pisso I., and Stohl A.: Source-receptor matrix calculation for deposited mass with the Lagrangian particle dispersion model FLEXPART v10.2 in backward mode. Geophys. Mod. Dev. 10, 4605-4618, doi:10.5194/gmd-10-4605-2017, 2017.

ECMWF: User Guide to ECMWF Products 2.1. Meteorological Bulletin M3.2. Reading, UK, 1995.

Emanuel, K. A., and Živković-Rothman, M.: Development and evaluation of a convection scheme for use in climate models. J. Atmos. Sci., 56, 1766–1782, 1999.

Fang, X., Shao, M., Stohl, A., Zhang, Q., Zheng, J., Guo, H., Wang, C., Wang, M., Ou, J., Thompson, R.L., and Prinn, R.G.: Top-down esti-
5   mates of benzene and toluene emissions in the Pearl River Delta and Hong Kong, China, Atmos. Chem. Phys. 16, 3369-3382, 10.5194/acp-16-3369-2016. 2016.

Flesch, T. K., Wilson, J. D., and Lee, E.: Backward-time Lagrangian stochastic dispersion models and their application to estimate gaseous emissions, J. Appl. Meteorol., 34, 1320–1333, 1995.

Forster, C., Wandinger, U., Wotawa, G., James, P., Mattis, I., Althausen, D., Simmonds, P., O'Doherty, S., Kleefeld, C., Jennings, S. G.,
10   Schneider, J., Trickl, T., Kreipl, S., Jäger, H., and Stohl, A.: Transport of boreal forest fire emissions from Canada to Europe. J. Geophys. Res., 106, 22,887–22,906, 2001.

Forster, C., Stohl, A., and Seibert, P.,: Parameterization of Convective Transport in a Lagrangian Particle Dispersion Model and Its Evaluation. J. Appl. Meteor. Climatol., 46, 403–422, 2007. https://doi.org/10.1175/JAM2470.1

Global Soil Data Task: Global soil data products CD-ROM contents (IGBP-DIS), Data Set, Oak Ridge Natl. Lab. Distrib. Active Arch. Cent.,
15   Oak Ridge, Tenn., doi:10.3334/ORNLDAAC/565, 2014.

Groot Zwaaftink, C.D., O. Arnalds, P. Dagsson-Waldhauserova, S. Eckhardt, J. M. Prospero, A. Stohl: Temporal and spatial variability of Icelandic dust emission and atmospheric transport, Atmospheric Chemistry and Physics, 17, 10865-10878, doi:10.5194/acp-17-10865-2017, 2017.

Groot Zwaaftink, C. D., Grythe, H., Skov, H., and Stohl, A.: Substantial contribution of northern high-latitude sources to mineral dust in the
20   Arctic, J. Geophys. Res.-Atmos., 121, 13678–13697, https://doi.org/10.1002/2016JD025482, 2016.

Groot Zwaaftink, C. D., Henne, S., Thompson, R. L., Dlugokencky, E. J., Machida, T., Paris, J.-D., Sasakawa, M., Segers, A., Sweeney, C., and Stohl, A.: Three-dimensional methane distribution simulated with FLEXPART 8-CTM-1.1 constrained with observation data, Geosci. Model Dev., 11, 4469-4487, https://doi.org/10.5194/gmd-11-4469-2018, 2018.

Grythe, H., Kristiansen, N. I., Groot Zwaaftink, C. D., Eckhardt, S., Tunved, P., Krejci, R., Ström, J., and Stohl, A. : A new aerosol wet
25   removal scheme for the Lagrangian particle model FLEXPART v10. Geosci. Model Dev., 10, 1447-1466, doi:10.5194/gmd-10-1447-2017, 2017.

Heinz, S.: Statistical Mechanics of Turbulent Flows, Springer, Berlin, Heidelberg, Germany, 214 pp., 2003.

Henne, S., Brunner, D., Oney, B., Leuenberger, M., Eugster, W., Bamberger, I., Meinhardt, F., Steinbacher, M., and Emmenegger, L.: Validation of the Swiss methane emission inventory by atmospheric observations and inverse modelling, Atmos. Chem. Phys., 16, 3683?3710,
30   doi:10.5194/acp-16-3683-2016, 2016.

Henning, S., Bojinski, S., Diehl, K., Ghan, S., Nyeki, S., Weingartner, E., Wurzler, S., and Baltensperger, U.: Aerosol partitioning in natural mixed-phase clouds, Geophys. Res. Lett., 31, L06101, doi:10.1029/2003GL019025, 2004.

Hertel, O., Christensen, J. Runge, E. H., Asman, W. A. H., Berkowicz, R., Hovmand, M. F. and Hov, O.: Development and testing of a new variable scale air pollution model - ACDEP. Atmos. Environ., 29, 1267–1290, 1995.

35   Hittmeir, S., Philipp, A., and Seibert, P.: A conservative reconstruction scheme for the interpolation of extensive quantities in the Lagrangian particle dispersion model FLEXPART. Geosci. Model Dev., 11, 2503-2523, https://doi.org/10.5194/gmd-11-2503-2018, 2018.

Hoyer, S. J. and Hamman, A. and Kleeman, C. and Fitzgerald, C. and Rocklin, M.: xarray: N-D labeled arrays and datasets in Python. in prep, J. Open Res. Software, 2016.

Jones, A., Thomson, D., Hort, M., and Devenish, B.: The UK Met Office's next generation atmospheric dispersion model, NAME III, in Air Pollution Modelling and its Application XVII, edited by C. Borrego and A.-L. Norman, pp. 580–589, Springer, New York, 2007.

Kok, J. F.: A scaling theory for the size distribution of emitted dust aerosols suggests climate models underestimate the size of the global dust cycle, P. Natl. Acad. Sci. USA, 108, 1016–1021, https://doi.org/10.1073/pnas.1014798108, 2011.

5 Kristiansen, N. I., Stohl, A., Prata, A. J., Richter, A., Eckhardt, S., Seibert, P., Hoffmann, A., Ritter, C., Bitar, L., Duck, T. J., and Stebel, K.: Remote sensing and inverse transport modelling of the Kasatochi eruption sulphur dioxide cloud, J. Geophys. Res., 115, D00L16, doi:10.1029/2009JD013286, 2010.

Kristiansen, N. I., Stohl, A., Prata, F., Bukowiecki, N., Dacre, H., Eckhardt, S., Henne, S., Hort, M., Johnson, B., Marenco, F., Neininger, B., Reitebuch, O., Seibert, P., Thomson, D., Webster, H., and Weinzierl, B.: Performance assessment of a volcanic ash transport model mini-ensemble used for inverse modelling of the 2010 Eyjafjallajökull eruption, J. Geophys. Res., 117, D00U11, doi:10.1029/2011JD016844, 2012.

Kristiansen, N. I., Prata, A. J., Stohl, A. and Carn, S. A. : Stratospheric volcanic ash emissions from the 13 February 2014 Kelut eruption. Geophys. Re. Lett. 42, 588-596, doi:10.1002/2014GL062307, 2015.

Kristiansen, N. I., Stohl, A., Olivié, D. J. L., Croft, B., Søvde, O. A., Klein, H., Christoudias, T., Kunkel, D., Leadbetter, S. J., Lee, Y. H., Zhang, K., Tsigaridis, K., Bergman, T., Evangeliou, N., Wang, H., Ma, P.-L., Easter, R. C., Rasch, P. J., Liu, X., Pitari, G., Di Genova, G., Zhao, S. Y., Balkanski, Y., Bauer, S. E., Faluvegi, G. S., Kokkola, H., Martin, R. V., Pierce, J. R., Schulz, M., Shindell, D., Tost, H., and Zhang, H.: Evaluation of observed and modelled aerosol lifetimes using radioactive tracers of opportunity and an ensemble of 19 global models, Atmos. Chem. Phys., 16, 3525-3561, doi:10.5194/acp-16-3525-2016, 2016.

Kyrö, E.-M., Grönholm, T., Vuollekoski, H., Virkkula, A., Kulmala, M., and Laakso, L. : Snow scavenging of ultrafine particles: field measurements and parameterization. Boreal Env. Res., 14, 527-538, 2009.

Laakso, L., Grönholm, T., Rannika, Ü., Kosmalea, M., Fiedlera, V., Vehkamäki, H., and Kulmala, M.: Ultrafine particle scavenging coefficients calculated from 6 years field measurements Atm. Env. 37, 3605-3613, doi:10.1016/S1352-2310(03)00326-1, 2003.

Laloyaux, P., de Boisseson, E., Balmaseda, M., Bidlot, J.R. Broennimann, S., Buizza, R., Dalhgren, P., Dee, D., Haimberger, L., Hersbach, H., Kosaka, Y., Martin, M., Poli, P., Rayner, N., Rustemeier, E., and Schepers, D.: CERA20C: A coupled reanalysis of the twentieth century. J. Adv. Mod. Earth Syst., 10, 1172-1195. https://doi.org/10.1029/2018MS001273, 2018.

Legras, B., Joseph, B., and Lefevre, F.: Vertical diffusivity in the lower stratosphere from Lagrangian back-trajectory J. Geophys. Res., 108, 4562, doi:10.1029/2002JD003045, 2003.

Lin, J. C., Gerbig, C., Wofsy, S. C., Andrews, A. E. , Daube, B. C. , Davis, K. J., and Grainger, C. A.: A near-field tool for simulating the upstream influence of atmospheric observations: The Stochastic Time-Inverted Lagrangian Transport (STILT) model, J. Geophys. Res., 108(D16), 4493, doi:10.1029/2002JD003161, 2003.

Luhar, A. K., and Britter, R. E.: Random walk model for dispersion in inhomogeneous turbulence in a convective boundary layer, Atm. Env. 23, 1911—1924, 1989.

Marticorena, B., and Bergametti, G.: Modeling the atmospheric dust cycle: 1. Design of a soil-derived dust emission scheme, J. Geophys.Res., 100, 16,415–16,430, doi:10.1029/95JD00690, 1995.

35 McConnell, J. R., Wilson, A. I., Stohl, A., Arienzo, M. M., Chellman, N. J., Eckhardt, S., Thompson, E. M., Pollard, A. M., and Steffensen, J. P.: Lead pollution recorded in Greenland ice indicates European emissions tracked plagues, wars, and imperial expansion during antiquity, Proc. Natl. Acad. Sci. 115, 5726-5731, doi:10.1073/pnas.1721818115, 2018.

McMahon, T. A., and Denison, P. J.: Empirical atmospheric deposition parameters - a survey. Atmos. Environ., 13, 571–585, 1979.

Moxnes, E., Kristiansen, N.I., Stohl, A., Clarisse, L., Durant, A., Weber, K., and Vogel, A.: Separation of ash and sulfur dioxide during the 2011 Grímsvötn eruption, J. Geophys. Res. Atmos., 119, 7477–7501, doi:10.1002/2013JD021129, 2014.

Message Passing Interface Forum, 2015. URL: https://www.mpi-forum.org/

Naeslund, E., and Thaning, L.: On the settling velocity in a nonstationary atmosphere. Aerosol Sci. Technol., 14, 247-256, 1991.

5 Oney, B., Henne, S., Gruber, N., Leuenberger, M., Bamberger, I., Eugster, W., and Brunner, D.: The CarboCount CH sites: characterization of a dense greenhouse gas observation network. Atmos. Chem. Phys., 15, 11147-11164, doi:10.5194/acp-15-11147-2015, 2015.

Ottino, J.: The Kinematics of Mixing: Stretching, Chaos and Transport. Cambridge Univ. Press, New York, 1989.

Pisso, I. and Legras, B.: Turbulent vertical diffusivity in the sub-tropical stratosphere, Atmos. Chem. Phys., 8, 697-707, https://doi.org/10.5194/acp-8-697-2008, 2008.

10 Ramli, H. M. and Esler, J. G.: Quantitative evaluation of numerical integration schemes for Lagrangian particle dispersion models, Geosci. Model Dev., 9, 2441-2457, doi:10.5194/gmd-9-2441-2016, 2016.

Rastigejev, Y., Park, R., Brenner, M., and Jacob, D.: Resolving intercontinental pollution plumes in global models of atmospheric transport, J. Geophys. Res., 115, D02302, doi:10.1029/2009JD012568, 2010.

Reithmeier, C. and Sausen, R.: ATTILA: Atmospheric Tracer Transport in a Lagrangian Model, Tellus B, 54, 278–299, 2002.

15 Rodean, H.: Stochastic Lagrangian models of turbulent diffusion, Meteorological Monographs, 26 (48). American Meteorological Society, Boston, USA, 1996.

Seibert, P., and Frank, A.: Source-receptor matrix calculation with a Lagrangian particle dispersion model in backward mode, Atmos. Chem. Phys., 4, 51–63, 2004.

Seibert, P., Krüger, B., and Frank, A.: parametrisation of convective mixing in a Lagrangian particle dispersion model, Proceedings of the 20 5th GLOREAM Workshop, Wengen, Switzerland, September 24–26, 2001.

Shao, Y., and Lu, H.: A simple expression for wind erosion threshold friction velocity, J. Geophys. Res., 105, 22,437–22,443, doi:10.1029/2000JD900304, 2000.

Sodemann, H., Lai,T. M., Marenco, F., Ryder, C. L., Flamant, C., Knippertz, P., Rosenberg, P., Bart, M., and McQuaid, J. B.: Lagrangian dust model simulations for a case of moist convective dust emission and transport in the western Sahara region during Fennec/LADUNEX, J. 25 Geophys. Res. Atmos., 120, 6117?6144, doi:10.1002/2015JD023283., 2015.

Spichtinger, N., Wenig, M., James, P., Wagner, T., Platt, U., and Stohl, A.: Satellite detection of a continental-scale plume of nitrogen oxides from boreal forest fires, Geophys. Res. Lett., 28, 4579–4582, 2001.

Stein, A.F., Draxler, R.R, Rolph, G.D., Stunder, B.J.B., Cohen, M.D., and Ngan, F.: NOAA's HYSPLIT atmospheric transport and dispersion modeling system, Bull. Amer. Meteor. Soc., 96, 2059-2077, http://dx.doi.org/10.1175/BAMS-D-14-00110, 2015.

30 Stohl, A.: Computation, accuracy and applications of trajectories – a review and bibliography. Atmos. Environ., 32, 947–966, 1998.

Stohl, A., Wotawa, G., Seibert, P., and Kromp-Kolb, H.: Interpolation errors in wind fields as a function of spatial and temporal resolution and their impact on different types of kinematic trajectories. J. Appl. Meteor., 34, 2149–2165, 1995.

Stohl, A., Hittenberger, M., and Wotawa, G.: Validation of the Lagrangian particle dispersion model FLEXPART against large scale tracer experiment data. Atmos. Environ., 32, 4245–4264, 1998.

35 Stohl, A., and Thomson, D. J.: A density correction for Lagrangian particle dispersion models. Bound.-Layer Met., 90, 155–167, 1999.

Stohl, A., and Trickl, T.: A textbook example of long-range transport: Simultaneous observation of ozone maxima of stratospheric and North American origin in the free troposphere over Europe, J. Geophys. Res., 104, 30,445–30,462, 1999.

Stohl, A., Haimberger, L., Scheele, M.P., and Wernli, H.: An intercomparison of results from three trajectory models. Meteorol. Applications, 8, 127-135, 2001.

Stohl, A., Eckhardt, S., Forster, C., James, P., Spichtinger, N., and Seibert, P.: A replacement for simple back trajectory calculations in the interpretation of atmospheric trace substance measurements. Atmos. Environ., 36, 4635–4648, 2002.

5   Stohl, A., Forster, C., Eckhardt, S., Spichtinger, N., Huntrieser, H., Heland, J., Schlager, H., Wilhelm, S., Arnold, F., and Cooper, O.: A backward modeling study of intercontinental pollution transport using aircraft measurements. J. Geophys. Res., 108, 4370, doi:10.1029/2002JD002862, 2003.

Stohl, A., Cooper, O. R., Damoah, R., Fehsenfeld, F. C., Forster, C., Hsie, E.-Y., Hubler, G., Parrish, D. D,. and Trainer, M.: Forecasting for a Lagrangian aircraft campaign. Atmos. Chem. Phys., 4, 1113–1124, 2004.

10 Stohl, A., and James, P.: A Lagrangian analysis of the atmospheric branch of the global water cycle: 1. Method description, validation, and demonstration for the August 2002 flooding in Central Europe. J. Hydrometeor. 5, 656–678, 2005.

Stohl, A., Seibert, P., Arduini, J., Eckhardt, S., Fraser, P., Greally, B. R., Lunder, C., Maione, M., Mühle, J., O'Doherty, S., Prinn, R. G., Reimann, S., Saito, T., Schmidbauer, N., Simmonds, P. G., Vollmer, M. K., Weiss, R. F., and Yokouchi, Y.: An analytical inversion method for determining regional and global emissions of greenhouse gases: Sensitivity studies and application to halocarbons, Atmos. Chem.
15 Phys., 9, 1597-1620, https://doi.org/10.5194/acp-9-1597-2009, 2009.

Stohl, A., Forster, C., Frank, A., Seibert, P., and Wotawa, G.: Technical note: The Lagrangian particle dispersion model FLEXPART version 6.2., Atmos. Chem. Phys., 5, 2461-2474, 2005.

Stohl, A., Prata, A. J., Eckhardt, S., Clarisse, L., Durant, A., Henne, S., Kristiansen, N.I., Minikin, A., Schumann, U., Seibert, P., Stebel, K., Thomas, H. E., Thorsteinsson, T., Tørseth, K., and Weinzierl, B.: Determination of time- and height-resolved volcanic ash emissions and
20 their use for quantitative ash dispersion modeling: the 2010 Eyjafjallajökull eruption. Atmos. Chem. Phys. 11, 4333-4351, 2011.

Stohl, A., Seibert, P., Wotawa, G., Arnold, D., Burkhart, J. F., Eckhardt, S., Tapia, C., Vargas, A., and Yasunari, T. J.: Xenon-133 and caesium-137 releases into the atmosphere from the Fukushima Dai-ichi nuclear power plant: determination of the source term, atmospheric dispersion, and deposition. Atmos. Chem. Phys. 12, 2313-2343, doi:10.5194/acp-12-2313-2012, 2012.

Stohl, A., Klimont, Z., Eckhardt, S., Kupiainen, K., Shevchenko, V. P., Kopeikin, V. M., and Novigatsky, A. N.: Black carbon in the Arctic:
25 the underestimated role of gas flaring and residential combustion emissions. Atmos. Chem. Phys. 13, 8833-8855, doi: 10.5194/acp-13-8833-2013.244, 2013.

Stull, R. B.: An Introduction to Boundary Layer Meteorology. Kluwer Academic Publishers, Dordrecht, 1988.

Sutherland, W. : The viscosity of gases and molecular force, Philosophical Magazine, S. 5, 36, pp. 507-531, 1893.

Tateishi, R., N. T. Hoan, T. Kobayashi, B. Alsaaideh, G. Tana, and D. X. Phong: Production of Global Land Cover Data-GLCNMO2008, J.
30 Geogr. Geol., 6(3), 99, 2014.

Tegen, I., and I. Fung: Modeling of mineral dust in the atmosphere: Sources, transport, and optical thickness, J. Geophys. Res., 99(D11), 22,897–22,914, doi:10.1029/94JD01928, 1994.

Tiedtke, M.: Representation of clouds in large-scale models. Mon. Wea. Rev., 121, 3040-3061, 1993.

Thompson, R. L., and Stohl, A.: FLEXINVERT: an atmospheric Bayesian inversion framework for determining surface fluxes of trace species
35 using an optimized grid, Geosci. Model Dev., 7, 2223- 2242, doi:10.5194/gmd-7-2223-2014, 2014.

Thompson, R. L., Stohl, A., Zhou, L. X., Dlugokencky, E., Fukuyama, Y., Tohjima, Y., Kim, S.-Y., Lee, H., Nisbet, E. G., Fisher, R. E., Lowry, D., Zhao, G., Weiss, R. F., Prinn, R. G., O'Doherty, S., Fraser, P., and White, J. W. C.: Methane emissions in East Asia for 2000 - 2011 estimated using an atmospheric Bayesian inversion, J. Geophys. Res., 120, 9, 4352-4369, doi:10.1002/ 2014JD022394, 2015.

Thompson, R. L., Sasakawa, M., Machida, T., Aalto, T., Worthy, D., Lavric, J. V., Lund Myhre, C., and Stohl, A.: Methane fluxes in the high northern latitudes for 2005–2013 estimated using a Bayesian atmospheric inversion, Atmos. Chem. Phys., 17, 3553-3572, https://doi.org/10.5194/acp-17-3553-2017, 2017.

Thomson D.J. and Wilson J.D.: History of Lagrangian stochastic models for turbulent dispersion. In: Lin J, Brunner D, Gerbig C, Stohl A,
5   Luhar A, Webleyv P (eds.) Lagrangian modelling of the atmosphere. American Geophysical Union, Washington, DC, 2013.

Thomson D. J.: Criteria for the selection of stochastic models of particle trajectories in turbulent flows. J. Fluid Mech., 180, 529–556, 1987.

Thomson D.J.: A stochastic model for the motion of particle pairs in isotropic high-Reynolds-number turbulence, and its application to the problem of concentration variance. J. Fluid Mech 210:113?153, 1990.

Uliasz, M.: Lagrangian particle dispersion modeling in mesoscale applications. In: Zannetti, P. (ed.): *Environmental Modeling, Vol. II*. Com-
10   putational Mechanics Publications, Southampton, UK, 1994.

Verheggen, B., Cozic, J., Weingartner, E., Bower, K., Mertes, S., Connolly, P., Gallagher, M., Flynn, M., Choularton, T., and Bal-
tensperger, U. : Aerosol partitioning between the interstitial and the condensed phase in mixed phase clouds, J. Geophys. Res., 112: doi: 10.1029/2007JD008714, 2007.

Venkatram, A., and Wyngaard, J. C. (Eds.): Lectures on Air Pollution Modeling. American Meteorological Society, ISBN 9780933876675,
15   390 pp., Boston, 1988.

Weil, J.C., Updating Applied Diffusion Models, Venkatram, A., and Wyngaard, J. C. (Eds.): Lectures on Air Pollution Modeling, Journal of Applied Meteorology and Climatology, 1985. https://doi.org/10.1175/1520-0450(1985)024

Wilson, J. D., Thurtell, G. W., and Kidd, G. E.: Numerical simulation of particle trajectories in inhomogeneous turbulence part II: Systems with variable turbulence velocity scale. Bound.-Layer Met., 21, 423–441, 1981.

20 Wilson, J. D., and Sawford, B. L.: Review of Lagrangian stochastic models for trajectories in the turbulent atmosphere. Bound.-Layer Met., 78, 191–210, 1996.

Wotawa, G., L.-E. DeGeer, P. Denier, M. Kalinowski, H. Toivonen, R. D'Amours, F. Desiato, J.-P. Issartel, M. Langer, P. Seibert, A. Frank, C. Sloan, and H. Yamazawa (2003), Atmospheric transport modelling in support of CTBT verification – overview and basic concepts. Atmos. Environ., 37 (18), 2529–2537.

25 Zannetti, P.: Particle Modeling and Its Application for Simulating Air Pollution Phenomena. In: Melli P. and P. Zannetti (ed.): Environmental Modelling. Computational Mechanics Publications, Southampton, UK, 1992.